Appendix 2.4 A

Task 2.4 A: Salinity Removal Technologies

Submitted by:

Christopher J. Gabelich, Tae I. Yun, and James F. Green
Metropolitan Water District of Southern California
La Verne, California

Submitted to:

California Energy Commission
Sacramento, California

January 2002

LEGAL NOTICE

ACKNOWLEDGMENTS

Funding for this project was graciously provided by the California Energy Commission's Public Interest Energy Research Program. The authors wish to express their appreciation for the project management by Lory L. Larson, Southern California Edison. Technical and moral support were provided by Craig R. Bartels and Bradley M. Coffey, Metropolitan Water District of Southern California, La Verne, California.

The authors are also indebted to the student interns, Rafael Becerra, Monique Valenzuela, and Erica Wolski, who conducted the routine sampling and database management for the pilot-scale membrane processes. Special thanks to the students from Harvey Mudd College, Claremont, Calif. for conducting the pilot-scale membrane screening tests. Without their tireless efforts, this project would not have been a success. Additional thanks are extended to the entire Water Quality Laboratory staff at Metropolitan who set up and maintained the research platforms, and collected the data used during this study.

TABLE OF CONTENTS

List of Tables and Figures v
Preface vii
Executive Summary viii
Abstract xv
Introduction 1
Background 1
Project Objectives 5
Project Approach 5
Pilot-Scale Test Equipment 5
Economic Evaluation 6
Bench-Scale Test Equipment 7
Analytical Methods 9
Project Outcomes 10
Pilot-Scale Evaluation of Reverse Osmosis and Nanofiltration Membranes 10
Economic Evaluation of Reverse Osmosis and Nanofiltration Membranes 14
Evaluation of Commercial and Generic Antiscalants 16
Conclusions and Recommendations 28
General Conclusions 28
Commercialization Potential 30
Recommendations 30
Benefits to California 31
References 32
Glossary 34
Tables and Figures 36
Appendix A 69
Inorganic Constituents 69
Microbacteriological Methods 70
Appendix B 71

LIST OF TABLES AND FIGURES

Table 1. Basic properties of membrane processes 36
Table 2. List of commercial test membranes 36
Table 3. Nanofiltration membrane test matrix 37
Table 4. Commercial and generic antiscalant test matrix 38
Table 5. Summary of Membrane Performance 39
Table 6. Salinity removal of nanofiltration membranes 40
Table 7. Ionic and hydrated radii of common ions found in natural waters 41
Table 8. Qualitative effect of membrane productivity and salt rejection on system cost 41
Table 9. Economic evaluation of experimental membranes for a 300-mgd, split-flow-desalting plant to meet 500 mg/L TDS finished water quality goal 42
Table 10. Reference guide for bench-scale antiscalant testing 43
Table 11. Chemical and physical information for commercial antiscalants used in bench-scale testing. 44
Table 12. SEM results of fouled membrane surface of bench scale testing 45
Table 13. EDS results from membrane and colloidal analysis of bench scale testing 46
Table 14. EDS data of colloidal material from brine stream using CRW and 170 µg/L aluminum 47
Table 15. EDS data from RO membranes using CRW and 170 µg/L aluminum 47

Figure 1. Qualitative concept of high-pressure membrane separation processes 48
Figure 2. Polymer structure of polyamide membranes 48
Figure 3. Schematic drawing of pilot-scale membrane test unit 49
Figure 4. Large-scale, split-flow desalination cost model 50
Figure 5. Schematic drawing of bench-scale membrane test unit 51
Figure 6. Relationship of specific flux and salt rejection for nanofiltration membranes 51
Figure 7. Effect of water recovery on nanofiltration membrane flux 52
Figure 8. Effect of water recovery on nanofiltration membrane rejection 52
Figure 9. Effect of hydrated radius on nanofiltration membrane salt rejection 53

Figure 10. Effect of pH on membrane flux 54
Figure 11. Effect of pH on salt rejection 54
Figure 12. Specific permeate flux for citric acid using CRW/SPW 55
Figure 13. Specific permeate flux for salicylic acid using CRW/SPW 55
Figure 14. Specific permeate flux for EDTA using CRW/SPW 56
Figure 15. Specific permeate flux for commercial antiscalants using CRW/SPW 56
Figure 16. Specific permeate flux for commercial antiscalants using CRW at pH 8.3 57
Figure 17. Specific permeate flux for commercial antiscalants using CRW at pH 7.0 57
Figure 18. Specific permeate flux for generic antiscalants using CRW/SPW 58
Figure 19. Specific permeate flux for generic antiscalants using CRW at pH 8.3 58
Figure 20. Specific permeate flux for generic antiscalants using CRW at pH 7.0 59
Figure 21. Maximum permeate flux decline of commercial and generic antiscalants in three types of waters in RO bench-scale testing. 60
Figure 22. Dissolved calcium in RO concentrate for commercial and generic antiscalants in bench-scale testing. 61
Figure 23. Dissolved barium in RO concentrate for commercial and generic antiscalants in bench-scale testing. 62
Figure 24. SEM micrograph of a cleaned reverse osmosis membrane 63
Figure 25. Representative SEM micrographs of fouled reverse osmosis membranes from bench-scale testing 63
Figure 26. Dissolved silica in RO concentrate for commercial and generic antiscalants in bench-scale testing. 64
Figure 27. Dissolved aluminum in RO concentrate for commercial and generic antiscalants in bench-scale testing. 65
Figure 28. Specific permeate flux for commercial and generic antiscalants using CRW at pH 6.7 with 170 µg/L added aluminum 66
Figure 29. Dissolved analytes in RO concentrate for commercial, generic and blends of commercial and generic antiscalants in bench-scale testing with 170 µg/L added aluminum. 67
Figure 30. SEM micrographs of fouled reverse osmosis membranes from the aluminum addition study 68

PREFACE

The Public Interest Energy Research (PIER) Program supports public interest energy research and development that will help improve the quality of life in California by bringing environmentally safe, affordable, and reliable energy services and products to the marketplace.

The PIER Program, managed by the California Energy Commission (Commission), annually awards up to $62 million to conduct the most promising public interest energy research by partnering with Research, Development, and Demonstration (RD&D) organizations, including individuals, businesses, utilities, and public or private research institutions.

PIER funding efforts are focused on the following six RD&D program areas:

- Buildings End-Use Energy Efficiency
- Industrial/Agricultural/Water End-Use Energy efficiency
- Renewable Energy
- Environmentally-Preferred Advanced Generation
- Energy-Related Environmental Research
- Strategic Energy Research

What follows is the final report for *Electrotechnology Applications for Potable Water Production and Protection of the Environment*, Contract No. 500-97-044**,** conducted by the Metropolitan Water District of Southern California. The report is entitled "Electrotechnology Applications for Potable Water Production and Protection of the Environment: Task 4 Salinity Removal Technologies." This project contributes to the Industrial/Agricultural/Water End-Use Energy Efficiency area.

For more information on the PIER Program, please visit the Commission's Web site at: http://www.energy.ca.gov/research/index/html or contact the Commission's Publications Unit at 916-654-5200.

EXECUTIVE SUMMARY

Introduction

In order to aid State municipalities in desalination of various water sources, this project was conducted as part of the Desalination Research and Innovation Partnership (DRIP) managed by the Metropolitan Water District of Southern California (Metropolitan). Various reverse osmosis (RO) and nanofiltration (NF) membranes were evaluated in terms of membrane water production, salt rejection, pressure requirements, and long-term performance. Additionally, various commercial and generic antiscalants were evaluated for their effectiveness in preventing scale formation in membrane processes treating Colorado River water at high water recovery. This research may be applicable to other surface water supplies and will assist municipalities to minimize the cost of salinity reduction.

Background

Both RO and NF membranes can remove inorganic salts, as well as nearly all bacteria, viruses, and other particles that pass through the pretreatment process. However, differences in polymer chemistries lead to varying salt rejection and water production characteristics for each membrane type. This project sought to test various commercially available RO and NF membranes to determine the optimal membrane type for desalting Colorado River water, i.e., high salt removal, high membrane flux, and low applied feed pressure.

The unique properties of RO membranes to reject inorganic species while passing relatively pure water has lead to the widespread use of membrane processes to treat various water sources. When excessive water is passed through the membrane (i.e., the water recovery is too high), this concentration process continues until a limiting salt exceeds its solubility and scaling occurs (Taylor and Jacobs 1996). Scaling reduces membrane productivity and limits water recovery within the membrane system. As a result, scaling is an important consideration in the operation of RO membranes.

For Colorado River water desalination, common fouling concerns include traditional scalants such as barium sulfate, calcium carbonate, as well as a non-traditional scalant, aluminum

silicates. While control strategies for calcium carbonate are well understood (e.g., pH adjustment), scale control methods for the remaining scalants are poorly understood and require empirical testing to validate scale inhibition properties.

Project Objectives

The objectives were:

1. Investigate the performance of experimental RO membranes and NF membranes. Low-fouling and low-energy RO and NF membranes were evaluated to determine flux and selectivity for Colorado River water desalting;

2. Evaluate the long-term fouling rate of RO membranes using conventionally pretreated water. Cleaning frequency, and flux recovery after chemical cleaning were characterized. Reverse osmosis elements from three different manufacturers were evaluated to determine their potential for fouling;

3. Determine potential cost savings using experimental membrane flux and salt rejection data; and

4. Evaluate various commercial and generic antiscalants to prevent scale formation during RO treatment of Colorado River water.

Project Approach

Commercial Membrane Testing

A total of five RO membranes (four experimental [RO1, RO3 through RO5] and one commercially available [RO2]) were evaluated on the pilot-scale using conventional treatment with either aluminum sulfate or ferric chloride coagulation as the pretreatment step. The RO membranes were operated to gauge not only water production (specific flux) and salt rejection characteristics of the membranes, but their fouling behavior using conventionally treated water. Data collected during these tests included flows, pressures, conductivity, and water quality.

In addition to RO membranes, a total of seven experimental NF membranes were evaluated. Each experiment was run using a closed-loop, membrane-test unit until steady-state performance conditions were reached (approximately 3 to 5 days). In addition to evaluating specific flux and salt rejection of each membrane, several membranes were tested to determine the effects of changing salinity, pH, and ion size on salt rejection. Data collection was similar to that during RO testing.

Commercial and Generic Antiscalant Testing

Eight commercial antiscalants and six generic antiscalants were evaluated on the bench-scale to determine their efficacy for scale inhibition. The dosage for each commercial antiscalant was determined using the antiscalant vender's software and Colorado River water quality data. The chemical dosage for each of the generic antiscalants was based on published data and stoichiometric modeling. Each antiscalant was evaluated using a closed-loop, bench-scale test unit using spiral-wound RO membranes at 95 percent water recovery to enhance scale formation. The water quality data of the pretreatment and RO processes were collected in the form of hardness, alkalinity, TDS, major cations and anions, trace metals, particle count, turbidity, temperature, and pH. Additional data collected included feed and concentrate flows and pressures, influent and effluent conductivity, and scanning electron microscopy (SEM) and energy dispersive spectroscopy (EDS) of the membrane surface.

Project Outcomes

Pilot-Scale Evaluation of Reverse Osmosis and Nanofiltration Membranes

Table ES1 provides a summary of the operating parameters for the membranes tested during this study. Of the five RO membranes evaluated during this study, RO1 (Dow Separation Processes, FilmTec Enhanced LE) provided the highest specific flux (0.37 gfd/psi) while still maintaining high salt rejection (98.8 percent). Performance data for NF membranes provided a wider range of variation in water production and salt rejection properties than RO membranes. While NF membranes generally provided high specific flux and lower salt rejection than the RO membranes tested, membrane NF1 (Dow Separation Processes,

FilmTec NF90) showed comparable specific flux and salt rejection (0.36 gfd/psi and 98.6 percent, respectively) to that of RO1.

Ion hydrated radius and solution pH had a direct impact on the salt rejection behavior of NF membranes. Generally, as the hydrated radius increased (e.g., from sodium to sulfate), the rejection of that ion also increased. Additionally, operation at low pH conditions increased NF membrane salt rejection through chemically tightening of the membrane surface.

Economic Evaluation of Reverse Osmosis and Nanofiltration Membranes

When compared against a currently available commercial RO membrane (RO2), each of the four experimental RO membranes studied lowered overall membrane systems costs by at least 15 percent. Therefore, the project goal to reduce the membrane systems cost by 10 percent was met. Of the RO membranes tested, RO1 demonstrated the highest specific flux (0.37 gfd/psi) while still maintaining excellent salt rejection (98.8 percent). These two factors resulted in RO1 showing the greatest cost savings (20 percent) over current commercial RO membranes. Two of the NF membranes tested (NF1 and NF7) demonstrated superior performance in terms of both specific flux and salt rejection over a current commercially available ultra-low-pressure RO membrane, resulting in a 19 and 14 percent cost savings, respectively.

In order to minimize the capital and O&M costs for a membrane system, membrane selection plays a vital role. The effects of inherent membrane properties are two fold: (1) as operating pressure decreases, so too does the operation and maintenance (O&M) cost component due to reduced energy consumption; and (2) as salt rejection increases, the capital cost component decreases due to less treated water needing to be blended to achieve the target TDS value. However, the ultimate selection of an appropriate membrane is predicated on the specific application's water quality and quantity goals.

Evaluation of Commercial and Generic Antiscalants

The primary scalants of concern were calcium carbonate and barium sulfate. The degree of scaling from these constituents was predicated on source water quality and the water

recovery. A secondary scalant/foulant of concern was aluminum silicates. Selection of the appropriate antiscalant is predicated on influent water quality, pretreatment type, and system water recovery.

For Colorado River water, phosphonate-based antiscalants performed well at 85 percent water recovery. A potential mitigation strategy for aluminum silicate scale formation is through the use of complexing agents to bind with the dissolved aluminum. Potential aluminum complexing agents include citric acid and EDTA. Bench-scale experiments confirmed that both citric acid and EDTA might be effective in preventing the aluminum silicate scales. However, when both citrate (chemically similar to citric acid) and EDTA were used in tandem with a phosphonate-based antiscalant, aluminum silicate fouling was observed. The phosphate component of the commercial antiscalant may have reacted with the dissolved aluminum to form an aluminum phosphate foulant, which may serve as an intermediate step towards aluminum silicate fouling.

Conclusions and Recommendations

With the development of polyamide membranes, not only has the operating pressures for membrane systems decreased, but the water production per psi has also increased substantially. However, future increases in energy savings will not be as dramatic due to the approaching physiochemical limits for driving pressure. Currently, NF membranes operate at significantly higher flux rates than RO membranes, but exhibit poorer salt rejection. Further research is needed to wed the high water production of NF membranes with the high salt rejection of RO membranes. Additional research is needed to develop next generation membranes such that they are either chlorine tolerant to prevent biofouling or exhibit unique surface charge characteristics that prevent particle and bacterial adhesion, or even scaling.

This project only evaluated a small fraction of the total number of antiscalant types available for municipal water treatment. In order to facilitate information exchange between research groups, a standardized antiscalant test protocol needs to be developed. A primary concern with antiscalant testing is achieving representative water quality conditions that mimic those found in full-scale treatment plants at a given water recovery. Closed-loop membrane testing, while inexpensive, may not provide representative water quality conditions and

single-pass, multi-array membrane systems are not only expensive but have high water flow rate demands (up to 20 gpm). Therefore, smaller, single-pass membrane test systems need to be developed. Additionally, a standardized protocol for interpreting RO membrane and water quality data to judge antiscalant effectiveness needs to be developed

Table ES1. Summary of Membrane Performance

Code	Membrane	Normalized Flux (gfd)*	Specific Flux (gfd/psi)	Nominal Salt Rejection (percent)†
Reverse Osmosis Membranes‡				
RO1	FilmTec Enhanced LE	20.5	0.37	98.8
RO2	Koch Fluid Systems TFC-ULP®	16.4	0.22	93.9
RO3	Hydranautics LFC1	12.2	0.20	98.6
RO4	Hydranautics ESPA3	18.7	0.26	99.1
RO5§	Hydranautics ESPA1	14.5	0.21	99.0
*Nanofiltration Membranes***				
NF1	FilmTec NF90	23.2	0.36	98.6
NF2	FilmTec NF200	18.0	0.24	82.3
NF3	Hydranautics Prototype CTC50	24.7	0.44	54.5
NF4	Koch Fluid Systems SR1	24.5	0.30	64.5
NF5	Koch Fluid Systems SR2	25.6	0.63	52.5
NF6	TriSep TS80-TSA	21.8	0.28	62.6
NF7	TriSep XN40-TZF	18.8	0.24	97.8

* Normalized to 25ºC
† As measured by conductivity
‡ Pretreated using conventional treatment with alum
§ Pretreated using conventional treatment with ferric chloride
** Pretreated using microfiltration

ABSTRACT

In order to aid State municipalities in desalination of various water sources, this project was conducted as part of the Desalination Research and Innovation Partnership (DRIP) managed by the Metropolitan Water District of Southern California. Various experimental and commercial reverse osmosis (RO) and nanofiltration (NF) membranes were evaluated in terms of membrane water production per unit of pressure, and salt rejection. Additionally, various commercial and generic antiscalants were evaluated for their effectiveness in preventing scale formation in membrane processes treating Colorado River water at high water recovery. Specific flux and salt rejection of the membranes tested ranged from 0.20 to 0.37 gallon/ft^2/day/psi (gfd/psi) and 94 to 99 percent rejection of total dissolved solids (TDS) for RO membranes, respectively, and 0.24 to 0.63 gfd/psi and 53 to 99 percent rejection of TDS for NF membranes, respectively. Each of the four experimental RO membranes studied improved overall membrane system cost by at least 15 percent over a current commercially available ultra-low-pressure RO membrane. Additionally, two of the NF membranes tested (NF1 and NF7) demonstrated superior performance in terms of both specific flux and salt rejection, resulting in a 19 and 14 percent potential cost savings, respectively. Phosphonate-based antiscalants provided adequate protection for barium sulfate and calcium carbonate scalants at 85 percent water recovery; however, they may react with pretreatment coagulant residuals to aid in the formation of aluminum-based foulants.

INTRODUCTION

Membrane technologies have found wider acceptance in recent years. Prior to their implementation, bench- and pilot-scale testing should be undertaken to reveal any operational limitations or problems. Key considerations for the full-scale implementation of membrane processes (e.g., reverse osmosis [RO] and nanofiltration [NF]) are membrane water production, salt rejection, pressure requirements, and long-term performance. Towards that end, the Metropolitan Water District of Southern California (Metropolitan), in conjunction with its partners, initiated the Desalination Research and Innovation Partnership (DRIP) program to develop and evaluate new and innovative technologies to substantially reduce the cost of desalinating Colorado River water and other brackish sources. A major research area for the DRIP program is to evaluate current and experimental membrane products in an effort to increase water production, while still maintaining high salt rejection and low applied feed pressures.

This task evaluated various membrane manufacturer's products to more cost-effectively remove total dissolved solids (TDS), or salts, from Colorado River water. Colorado River water contains upwards of 700 milligrams per liter (mg/L) of TDS with potential increases to 750 mg/L of TDS in the near future. Both RO and NF membranes effectively remove TDS, but the salt removal and water production characteristics vary by product manufacturer and membrane type. Additionally, various scale prevention chemicals (antiscalants) were tested for their ability to allow for high water recovery rates during the desalination process. This research will assist municipalities to minimize the cost of salinity reduction and may also be applicable to other surface water supplies.

Background

Membrane Processes

Pressure-driven membrane processes can be broken down into two general classes; (1) low-pressure membrane filtration and (2) high-pressure membrane separation processes (see Table 1). The low-pressure membrane filtration processes such as microfiltration (MF) and ultrafiltration (UF) remove particulates, colloids, and high-molecular-weight soluble

species—depending on the pore size of the membrane—by a size exclusion mechanism (Jacangelo and Buckley 1996, Anselme and Jacobs 1996). Nominal pore sizes for MF and UF processes for municipal water treatment are approximately 0.1 to 0.5 µm and 0.01 to 0.1 µm, respectively, though the pore sizes vary by manufacturer and membrane polymer construction. Both MF and UF processes generally allow most inorganic species to pass and retain discrete particulate matter such as particle, bacteria, and some viruses.

While the low-pressure MF and UF processes are size exclusion processes, high-pressure membrane separation processes (RO and NF) can be described as diffusion-controlled processes in that mass transfer of ions through these membranes are diffusion controlled. Reverse osmosis membranes are capable of rejecting contaminants or particles with diameters as small as 0.0001 µm, whereas NF membranes can reject contaminants as small as 0.001 µm (Taylor and Jacobs 1996). Although to characterize both RO and NF membranes based on pore-size is misleading in that the membranes are made of tightly cross-linked polymer chains that have no pores per say, but rather allow contaminants to diffuse across the membrane surface (see Figure 1). Therefore, both RO and NF membranes can remove inorganic salts, as well as nearly all bacteria, viruses, and other particles that pass through UF and MF membranes.

Nanofiltration membranes differ from RO membranes by the substitution of an amide functional group with a carboxyl functional group (see Figure 2). This carboxyl group causes the NF lattice to be weaker, thus yielding a larger pore size than RO membranes. An additional result of the carboxyl-containing NF membranes is that NF membranes are more highly charged than RO membranes. Typically polyamide membranes contain a net negative charge, but positive charge-carrying membranes do exist. By altering the membrane chemistry (i.e., charge), the salt rejection capabilities can be tailored for specific applications.

Currently, for brackish water applications, ultra-low-pressure RO membranes typically operate at applied feed pressures between 125 to 200 psi, while NF membranes operate between 100 to 200 psi. For surface water applications, the amount of water that can be safely passed through the membrane without undue fouling, water production or flux, ranges from 10 to 15 gallons per square foot of membrane per day (gfd). Lastly, while the salt

rejection for polyamide RO membranes can be greater than 98 percent, the salt rejection for polyamide NF membranes are lower and vary depending on the polymer chemistry. This project sought to test various commercially available RO and NF membranes to determine the optimal membrane type for desalting Colorado River water, i.e., high salt removal, high membrane flux, and low applied feed pressure.

Precipitative Fouling

The unique properties of RO membranes to reject inorganic species while passing relatively pure water has lead to the widespread use of membrane processes to treat various water sources. When excessive water is passed through the membrane (i.e., the water recovery is too high), this concentration process continues until a limiting salt exceeds its solubility and scaling occurs (Taylor and Jacobs 1996). Scaling reduces membrane productivity and limits water recovery within the membrane system. As a result, scaling is an important consideration in the operation of RO membranes.

In general, salts composed of divalent ions (e.g., calcium sulfate) are typically less soluble than those composed of monovalent ions (e.g., sodium chloride). Therefore, those salts that are best retained by RO membranes are also those salts that have the greatest potential to precipitate onto the membrane. One mitigating factor to this phenomena is that many ions, such as magnesium or strontium, may not present in the feed water at sufficient concentrations to be of concern even when they are concentrated by a factor of 5 to 6 times.

Concentration of scale-forming species may occur due to two phenomena: (1) bulk concentration of salts as water permeating through the membrane is removed from the salt solution; and, (2) concentration polarization (Wiesner and Buckley 1996). Common foulants of concern include calcium, barium, magnesium, and other metals. Precipitates of these species are most commonly carbonates, sulfates, and hydroxides.

Once the salt solubility is exceeded, scale formation ensues. Scale formation involves three basic stages (Darton 1997):

1. Ions start to cluster near the membrane surface as proto-nuclei of up to 1000 atoms as the ion concentration increases;

2. The proto-nuclei grow as concentration increases and the ions start ordering themselves into regular shaped nuclei; and,

3. Finally, crystals are formed from the nuclei. Once formed, the crystals continue to grow indefinitely as long as the respective salt solubility limit is exceeded.

Strategies for avoiding precipitative scaling often include ways of reducing the concentration of either the anion or the cation portion of the ion pair of concern (Bersillon and Thompson 1996, Boffardi 1996, Darton 1997). For example, acid can be added to reduce the concentration of the anionic species such as hydroxide or carbonate that may precipitate with divalent ions (e.g., magnesium hydroxide and calcium carbonate). Lime-soda ash treatment or ion exchange pretreatment may remove the cation component of hardness scales. However these scale control methods typically require multiple pH adjustments and costly solids handling infrastructure.

Both acid addition and water softening processes do relatively little to control for sulfate based scale. In these cases, antiscalants must be used to impede precipitation. However, the chemistry of antiscalant effectiveness is more complicated and less understood. Antiscalant selection is important to prevent ions from precipitating out of solution. Scale inhibitors (antiscalants) function by one or more of the following mechanisms (Darton 1997):

1. Threshold effect: sub-stoichiometric amounts of antiscalant prevent the precipitation of salts that have exceeded their solubility limit;

2. Crystal distortion effect: interference to normal crystal growth thereby producing an irregular crystal structure with poor scale forming potential; and,

3. Dispersancy: a surface charge is placed on the crystal, thereby causing the crystals to repel one another.

Polyacrylates, phosphonates, and to a lesser extent hexametaphosphates are used to control a variety of scales. Often commercial antiscalants are proprietary formulations with a mixture of the above chemicals, as well as other surfactants and chemical agents. Therefore, antiscalant performance can only be determined empirically.

Project Objectives

The objectives were:

1. Investigate the performance of experimental RO membranes and NF membranes. Low-fouling and low-energy RO and NF membranes were evaluated to determine flux and selectivity for Colorado River water desalting;

2. Evaluate the long-term fouling rate of RO membranes using conventionally pretreated water;

3. Determine potential cost savings using experimental membrane flux and salt rejection data; and

4. Evaluate various commercial and generic antiscalants to prevent scale formation during RO treatment of Colorado River water.

PROJECT APPROACH

Pilot-Scale Test Equipment

Two-Element Membrane Test Unit

A two-element membrane test unit was pilot tested during this portion of the project (see Figure 3). Each of the two parallel pressure vessels housed a single 4-in. x 40-in. membrane element. This design facilitated simultaneous membrane testing. To prevent particulate and biological fouling, the source water was microfiltered (U.S. Memcor, 3M10C, Timonium, Maryland) prior to use within the RO unit. The source water was 60 percent Colorado River water and 40 percent California State Project water. Antiscalant (1.6 mg/L Pretreat 191,

Permacare, Fontana, Calif.) was added to the influent reservoir. For a complete list of membranes tested and their corresponding tracking code, see Table 2.

Each experiment was run until steady-state performance conditions were reached (approximately 3 to 5 days). Table 3 shows the test matrix used during NF membrane testing. The applied feed pressure was adjusted to maintain a constant permeate flow rate. With the exception of two tests, the temperature (approximately 65°F) and pH (pH 8.1) were kept constant. For two membranes the pH of the water was lowered to 6.5 and 4.8 with hydrochloric acid, in addition to testing at ambient pH. In order to simulate varying water recovery levels (e.g., 10, 50, 85, and 90 percent water recoveries), the concentrate flow was returned to the feed tank while a portion of the permeate was discarded. Throughout the experiment, the operating pressure and concentrate flow rate were kept constant (80 to 100 psi and 5 to 10 gpm, respectively). Permeate flow rate was recorded every hour. In addition to taking water quality data at the start and finish of each experiment, the feed, permeate, and concentrate temperature and conductivity were recorded daily.

Three-Element Membrane Test Unit

A pilot-scale unit with three parallel pressure vessels was used to evaluate RO membrane performance on conventionally treated water using alum and ferric coagulants. Reverse osmosis membranes tested included: Hydranautics LFC1, ESPA1, and ESPA 3, Hydranautics, Oceanside, Calif.; TFC-ULP®, Koch Fluid Systems, San Diego, Calif.; FilmTec LE, Dow Separation Processes, Minneapolis, Minn.. Antiscalant (1.6 mg/L Permatreat 191; Permacare, Fontana, Calif.) was used. Because the unit operated at low recoveries (approximately 10 to 15 percent), no pH adjustment was required. This system was used solely to evaluate the organic, biological, and/or colloidal fouling potential of conventionally treated water.

Economic Evaluation

Metropolitan developed a large-scale, desalting plant model for this project (see Figure 4). The model assumed that split flow treatment was used to achieve 500 mg/L TDS. For a detail description of the cost model, see Task 3 Solids Removal Technologies of this report.

The model has been incorporated into a Microsoft Excel® Spreadsheet to make the necessary calculations. Salt rejection, energy consumption, and cleaning requirements were based on experimental data collected during this study. The influent TDS was assumed to be 750 mg/L. This was chosen because of the agreement made by seven Colorado River basin states that the salinity below the Parker Dam will be at or below 747 mg/L of TDS (Colorado River Salinity Control Forum 1996). This standard was specified in section 303 of the Clean Water Act. Applied pressure was based on the average specific flux for each membrane, and was adjusted to an average temperature of 64ºF (18ºC).

A fixed RO brine disposal cost without brine treatment was assumed for all options. For the purposes of this task, the RO brine was assumed to be 15 percent of the RO process influent, and disposal consisted of building a 30 mile pipeline from the treatment plant to the ocean. The estimated cost of the brine line was $20.5 million. This cost did not assume any site-work, purchase of land, environmental clearance, or other contingencies that may increase the cost substantially. To meet water supply goals (300 mgd), additional water would have to be imported to compensate for the lost water associated with the brine disposal. Both the costs of the brine line ($20.5 million) and the make-up water ($5.1 million per year) remained fixed for all modeling runs.

It should be noted, in the strongest terms, that this level of water loss (approximately 18 mgd) would be unacceptable in the arid Southwest. Additionally, the cost of design and construction of a 3 ft diameter brine line would certainly be substantially higher than the $20.5 million cost cited above due to the environmental impact report process, legal issues associated with gaining either the necessary right-of-way or land, or other cost factors. Brine treatment technologies to reduce the total disposal volume are both expensive and energy intensive, and are beyond the scope of this project.

Bench-Scale Test Equipment

Source Water

Three source waters were used during this phase of testing: (1) a blend of 60 percent Colorado River water and 40 percent California State Water Project water at ambient pH

(pH 8.0); (2) 100 percent Colorado River water at ambient pH (pH 8.2); and (3) 100 percent Colorado River water at pH 7. The source water was pretreated prior to the RO unit by a 0.2 µm nominal pore size microfiltration membrane (Aqua Pro Membranes, Gardena, Calif.). A 2.0 to 2.5 mg/L chloramine residual was maintained in the MF influent (3:1 w/w ratio of chlorine to nitrogen). The TDS of the three source waters ranged from 450 mg/L to 550 mg/L. A 20-gallon reservoir was used to store the MF effluent prior to RO treatment. The pH was adjusted to pH 7.0 using sulfuric acid.

Bench-Scale Reverse Osmosis Unit

Three identical closed-loop, bench-scale RO units were used to test the effectiveness of selected commercial antiscalants (see Figure 5). The bench-scale RO testing used spiral-wound, thin-film-composite, polyamide membranes (Energy Saving Polyamide ESPA1-2012, Hydranautics, San Diego, Calif.). The dimensions of each element were 1.8 in. diameter by 12 in. long, with 5.0 ft^2 of membrane surface area per element. Prior to testing, each RO element was soaked in deionized water for 3 hrs. The RO elements were then flushed with 10 gallons of deionized water for one hour, followed by a second flush with deionized water for an additional three hours in order to equilibrate the permeate flux and salt rejection of the RO membranes under normal operating pressure (80 psi) and constant concentrate flow (0.16 gpm).

For each set of experimental variables (e.g., water type) an experimental control test was conducted. The experimental controls consisted of operating the RO unit at normal pressures and flow rates but without any antiscalant. Therefore, the scale formation without the presence of antiscalant in target water was evaluated.

For each experiment, the final water recovery was set at 95 percent in order to accelerate the scale formation. Throughout the experiment, the operating pressure and concentrate flow rate were maintained at set values (80 psi and 0.16 gpm, respectively). The RO unit only recycled the concentrate flow but discarded the permeate flow. For every three tests, however, one permeate flow was collected for water analysis. Ninety-five percent water recovery (from 20 gallons to 1 gallon) was typically reached within nine hours, as measured

by volume. Permeate flow rate was recorded every hour. The feed, permeate, and concentrate temperature and conductivity were also measured hourly. Once 95 percent water recovery was reached, the RO unit was shut down and the RO elements as well as the final concentrate were collected for analysis. All samples taken were stored in a refrigerator for further analyses. The unit was then flushed with tap water to remove any residual solution.

Antiscalants

Eight commercial antiscalants and six generic antiscalants were evaluated to determine their efficacy for scale inhibition (see Table 4). The dosage for each commercial antiscalant was calculated using the antiscalant vender's software and Colorado River water quality data. The chemical dosage for each of the generic antiscalants was based on published data and stoichiometric modeling. All commercial and generic antiscalants were added to the RO feed tank.

Analytical Methods

The water quality data of the pretreatment and RO processes were collected in the form of hardness, alkalinity, TDS, major cations and anions, trace metals, particle count, turbidity, temperature, and pH. For a complete list of analytical methods see Appendix A. All sampling was conducted by Metropolitan's staff. Inorganic and microbial analyses were analyzed at Metropolitan's Water Quality Laboratory in La Verne, CA.

Membrane Autopsy

Upon completion of each membrane test, the RO or NF element was autopsied by Metropolitan personnel. Swatches of membrane material were collected and sent to independent laboratories for microscopic analysis. The following analyses were conducted:

> Scanning Electron Microscopy (SEM) was conducted by the Scripps Oceanographic Institute in La Jolla, CA using a Cambridge Instruments Model 360 (Leo Electron Microscopy, Thornwood New York). Membrane samples were prepared for top surface views by cutting a small piece of membrane and then attaching it to an aluminum mount with double-stick tape. Cross-sections were prepared by fracturing

a small strip of the membrane while in a liquid nitrogen bath; this was also attached to an aluminum mount. The mounted sample was sputter-coated with a 30-nm layer of gold and palladium.

Energy Dispersive Spectroscopy (EDS) was conducted in concert with the SEM by the Scripps Oceanographic Institute (Oxford Instruments Model QX2000, Concord Mass.). The membrane sample for EDS analysis was attached to a graphite mount with graphite tape; there was no coating on the sample. This technique was used because graphite is not detected by EDS and does not interfere with atoms being measured in the sample.

Calculated Values

In order to assess the performance of the membrane processes, several key values were calculated based on raw process data. These calculated values include silt density index (SDI) for the pretreatment step, specific normalized flux, and salt rejection (see Appendix B).

PROJECT OUTCOMES

Pilot-Scale Evaluation of Reverse Osmosis and Nanofiltration Membranes

Table 5 provides a summary of the operating parameters of the membranes tested during this study. A total of five RO membranes and seven NF membranes were tested on a variety of pretreatment technologies. For a complete description of the effects of pretreatment on membrane performance, see the Task 3 Solids Removal chapter of this report. While the type of pretreatment had a drastic effect on membrane fouling and long-term performance, several general conclusions could still be made regarding the relative performance differences between membrane manufacturers and membrane type.

Reverse Osmosis Membranes

Of the RO membranes tested, RO1 demonstrated the highest specific flux (0.37 gfd/psi) while still maintaining excellent salt rejection (98.8 percent) (see Table 5). Two other RO membranes demonstrated superior salt rejection capabilities (99.0 and 99.1 percent for RO5

and RO4, respectively), though these membranes operated with at least 30 percent lower specific fluxes (0.21 and 0.26 gfd/psi for RO5 and RO4, respectively). Given the type of pretreatment (conventional treatment with alum or ferric chloride), each of the RO membranes tested, with the exception of RO3, exhibited equivalent fouling rates (see Task 3 Solids Removal for a more detailed discussion on the effects of pretreatment on membrane fouling).

Chemical cleaning with acid and caustic solutions restored membrane flux upon inorganic fouling during testing with conventional treatment and ferric chloride as pretreatment. However, salt rejection was not completely restored after chemical cleaning. This finding may have been caused by chemical degradation of the membrane surface during operation with conventional treatment as pretreatment (see Task 3 Solids Removal technologies for a complete description of membrane fouling episodes during conventional treatment).

While membrane RO3 exhibited the lowest specific flux of the RO membranes tested during this study, it was a low-fouling composite membrane that was designed to maintain constant specific flux over time in high-fouling environments. Initial testing at Metropolitan indicated that the rate of particulate fouling for RO3 using conventional treatment with alum as pretreatment was lower than that of traditional polyamide membranes (see Task 3 Solids Removal for a more detailed discussion on pretreatment characteristics and fouling behavior). Therefore, while requiring higher initial operating pressure to generate a set flux rate, low-fouling composite membranes (e.g., RO3) may provide for more stable membrane performance and ultimately result in lower energy consumption over time.

It should be noted that as the specific flux increases, that does not necessarily translate into lower operating pressure, but rather better water production per unit of pressure. In other words, there exists a fixed minimum operating pressure needed to overcome the inherent osmotic and hydraulic pressure losses across the membrane. Therefore, while reductions in future operating pressure may by minimal, the amount of water production at a given pressure may still improve.

Nanofiltration Membranes

Table 5 also shows the operational variables for the various NF membranes tested. On average, NF membranes demonstrated 30 percent higher specific flux and 25 percent lower salt rejection than RO membranes. However, two NF membranes (NF1 and NF7) exhibited both high salt rejection (98.6 and 97.8 percent, respectively) and high specific flux (0.36 and 0.24 gfd/psi, respectively). Therefore, these membranes (NF1 and NF7) behaved similarly to RO membranes despite their differing polymer chemistries. Table 6 lists the individual ion and other water quality parameter rejections for all seven NF membranes. Of the seven NF membranes tested, specific flux and salt rejection ranged from 0.24 to 0.63 gfd/psi and 52.5 to 98.6 percent, respectively. In general, as the specific flux increased, the salt rejection decreased (see Figure 6). Therefore, the selection of the appropriate NF membrane depends on whether either salt rejection or water production is more critical to the application.

Following are brief discussions on the effects of salinity, ion size, and pH on NF membrane performance.

Effect of Salinity on Membrane Performance

Tests conducted in single-pass mode using a single-element membrane test unit can only model the specific flux and salt rejection of the primary element in a full-scale membrane system. In order to determine how each individual membrane would perform under various salt concentrations (i.e., at different locations within a full-scale membrane treatment plant), a portion of the permeate was removed from the closed-loop system to simulate varying TDS levels. Six of the seven NF membranes maintained constant specific flux regardless of the TDS level; indicating that membrane flux was independent of salt concentration at TDS levels less than 5,000 mg/L (see Figure 7). In addition, salt rejection properties of the NF membranes were also independent of salt concentration (see Figure 8).

Effect of Hydrated Radius on Solute Rejection

The rejection of inorganic solutes by RO membranes has been observed to follow the lyotropic series (increasing rejection with increasing hydrated radius) (Wiesner and Buckley 1996). The

degree of hydration depends on the nature of the ion: smaller ions with high charges (e.g., SO_4^{2-}) show greater degree of hydration than larger ions with lower charges (e.g., NO_3^-). For a list of common ions found in natural water and their respective hydrated radius see Table 7. Within a given series of ions, the hydrated radius is generally inversely proportional to the unhydrated ionic radius (Weber 1972). For example, cation rejection for RO membranes should obey the following order:

$$Mg^{2+} > Ca^{2+} > Sr^{2+} > Ba^{2+} > Na^+ > K^+$$

For anions of interest, ion rejection should obey the following order:

$$SO_4^{2-} > Cl^- > Br^- > NO_3^-$$

These relationships are rough generalizations, but provide a useful tool for envisioning the rejection behavior of various solutes (Wiesner and Buckley 1996). However, the salt rejection behavior of NF membranes is not as well understood.

The effect of hydrated radius on solute rejection for nine different ions and three different NF membranes was examined (see Figure 9). The three membranes shown (NF1, NF2, and NF3) represented varying levels of salt rejection (98.6, 82.3, and 54.5 percent, respectively). Salt rejection for NF1 showed the least responsiveness to hydrated radius than the other two membranes. Given the high overall salt rejection (98.6 percent), this finding indicates that the membrane polymers are "tightly" woven, thus resulting in good salt rejection of most analytes. As the salt rejection decreases (e.g., NF2 and NF3), the membranes show a greater propensity to reject larger ions (e.g., SO_4^{2-}) and pass smaller ions (e.g., Cl^-). Additionally, ion hydrated radius had a greater effect on anion rejection than cation rejection due to the negative charge on the membrane surface and the need to maintain charge neutrality.

Effect of pH on Membrane Performance

Nanofiltration membranes have negatively charged surfaces and as acid is added to the feed water the carboxyl functional group of the membrane polymer becomes hydrated, thus resulting in a more tightly woven membrane surface. Therefore, as pH of the feed water decreases, salt rejection may improve. Several tests were run to evaluate salt rejection

characteristics of NF membranes at three pH levels (pH 4.8, 6.5, and 8.1). These lower pH values were within the operating ranges of the membranes tested (pH 4.0 to 11.0).

Figure 10 shows the specific flux for two different NF membranes (NF1 and NF2) at pH 8.1, 6.5, and 4.8. As the water recovery increased, the specific flux decreased due to the lowering of the feed water pH. At 85 percent water recovery, the pH of the concentrate typically decreases by approximately 0.5 log. Additionally, the salt rejection of both membranes increased with decreasing pH (see Figure 11). These data support the theory that as the NF membranes become more hydrated at lower pH, the membrane becomes more tightly woven (i.e., it requires more pressure to maintain a constant flux rate due to more energy being needed to push water across the membrane surface). However, pH adjustment (especially from pH 8.1 to 4.8) is expensive and the increase in salt rejection at lower pH is slight. Therefore, pH adjustment for the sole purpose to increase salt rejection may not be economical at full-scale, though pH adjustment is often required to prevent calcium carbonate scaling at high water recovery.

Economic Evaluation of Reverse Osmosis and Nanofiltration Membranes

In many water treatment applications, the need to meet TDS objectives (e.g., 500 mg/L TDS) does not necessitate treating the full stream. Therefore, partial, or split-flow, treatment is employed. Split-flow treatment reduces the capital expenditures for installing desalting equipment. The effects of inherent membrane properties are two fold: (1) as operating pressure decreases, so too does the operation and maintenance (O&M) cost component due to reduced energy consumption; and (2) as salt rejection increases, the capital cost component decreases due to the less treated water needing to be blended to achieve the target TDS value (see Table 8). Therefore in order to minimize the capital and O&M costs for a membrane system, membrane selection plays a vital role. However, the ultimate selection of an appropriate membrane is predicated on the specific application's water quality and quantity goals.

Table 9 shows an economic evaluation for a hypothetical, membrane desalting facility using the various RO and NF membranes from this study to produce a 500 mg/L TDS finished

water. The size of the membrane plant was based on a fixed water recovery of 85 percent. The baseline condition (RO2) was selected based on the membrane being commercially available and therefore representative of the state-of-the-art, as of the beginning of this project. All other membranes tested (RO1, RO3 through RO5, and NF1 through NF7) were experimental products not currently available on the commercial market. The goal of this task was to test new membrane products such that the total costs for the membrane portion of a 300-mgd split-flow desalting facility was reduced by 10 percent.

Each of the four experimental RO membranes studied (RO1, RO3, RO4, and RO5) improved overall membrane systems costs by at least 15 percent. Therefore, the project goal to reduce the membrane systems cost by 10 percent was met. Of the RO membranes tested, RO1 demonstrated the highest specific flux (0.37 gfd/psi) while still maintaining excellent salt rejection (98.8 percent) (see Table 9). These two factors resulted in RO1 showing the greatest cost savings (20 percent) over current commercial RO membranes. While RO4 and RO5 demonstrated superior salt rejection (greater than 99 percent) than RO1, these two membranes did not have the high specific flux rate of RO1. Therefore, while the capital cost improved slightly, the increased O&M costs due to higher energy usage overcame this advantage.

Of the NF membranes tested, two membranes (NF1 and NF7) provided superior performance in terms of both specific flux and salt rejection over RO2. These findings resulted in a 19 and 14 percent cost savings, respectively, over the commercial RO membrane (RO2). Other NF membranes (NF2 through NF6), however, exhibited low salt rejection (53 to 82 percent) such that they could not meet the 500 mg/L TDS goal at 85 percent water recovery despite treating the full plant flow (300 mgd). Therefore, membranes NF2 through NF6 may not be appropriate for Colorado River water desalting. However, these membranes may be used to further concentrate the brine stream from a desalting plant due to their unique salt rejection properties.

Evaluation of Commercial and Generic Antiscalants

This task conducted bench-scale membrane testing of commercial and generic antiscalants. Bench-scale testing was conducted with 1.8-in. [4.6 cm] diameter, spiral-wound RO elements using microfiltered (0.2 µm nominal pore size) pretreated water. For a complete description of the RO and MF units, see the Project Methods section of this report. The goal of this task was to determine the efficacy of various antiscalant products in controlling the primary scales (barium sulfate and calcium carbonate) and secondary scales (aluminum silicates) at greater than 85 percent water recovery.

To evaluate the performance of antiscalants for scale inhibition, permeate flux and salt rejection data were calculated per ASTM Standards (1987). While flux decline and salt rejection are good macroscopic indicators of impaired membrane performance, operational constraints of the bench-scale units limited their usefulness in this application. In short, as water recovery was increased by bleeding off the permeate stream, the osmotic pressure of the feed water increased resulting in a reduction in net driving pressure. This decrease in net driving pressure exerted a greater influence on normalized flux than the declining permeate flux. The end result was an increase in normalized flux at the higher water recovery levels (e.g., greater than 85 percent). Membrane failure may also play a role, but salt rejection data did not support this conclusion.

Therefore, due to the bench-scale nature of the tests and the minimal amount of the potential scalant mass, a series of microscopic analyses were performed to quantify scaling potential. Specifically, water quality analysis (e.g., calcium, barium, silica, and aluminum) of the brine filtrate, SEM and EDS analysis of the RO membrane surface, and visual and chemical analysis of the colloidal material in the RO concentrate were evaluated. Many foulant constituents, such as calcium and barium, undergo phase changes between soluble and insoluble forms depending on their solubility. When the brine is filtered through a 0.45 µm filter, the soluble material passes through the filter. Higher solubilization of foulant materials is an indication of effective antiscalant performance.

The performance of each antiscalant was compared versus a control. The controls were also compared with each other to evaluate the scaling potential of the three types of waters tested. Commercial antiscalants were selected for control of calcium, barium and silica scales, and generic antiscalants were selected for control of aluminum precipitation by complexing the aluminum primarily and not for any other constituents. For ease of data interpretation, each antiscalant was assigned a tracking code (see Table 10).

Screening Tests

Commercial antiscalants were dosed using manufacturer's guidelines. These products were proprietary formulations that ranged from polyphosphonates, polyacrylates, and other organic polymers (see Table 11). However, no such guidelines were available for the generic antiscalants. Therefore, a series of preliminary tests were run to determine the optimal dosage for the generic antiscalants. Given microfiltration (MF) pretreatment excellent particle removal characteristics and the short duration of the tests (9 hr), both biological and particulate fouling most likely would have minimal influences on flux behavior. Therefore, any flux decline was assumed to be through the inorganic or organic precipitation. Steady-state flux behavior presumably indicated of no fouling through better antiscalant performance.

For citric acid, a dose of 1200 mg/L (GC1.2) showed the greatest reduction in flux loss compared to both the control and other citric acid dosages (see Figure 12). However, given that the pH was reduced to pH 3.2, the effect of lowering the pH may have had a greater influence on membrane performance than the antiscalant. Both 2.0 mg/L and 12 mg/L citric acid doses were proven effective in improving RO flux performance. Therefore, the 2.0 mg/L citric acid dose was used in all subsequent testing. For both salicylic acid and EDTA, no observable change in flux behavior was observed (see Figure 13 and Figure 14). Therefore, conservative dose levels for both chemicals were used in all subsequent testing (12 mg/L for both salicylic acid [GC4.2] and EDTA [GC5.2]).

Flux Comparison for Commercial and Generic Antiscalants

Each commercial and generic antiscalant was tested on the bench scale without replication. Figures 15 through 20 present the percent change in normalized flux at various water recoveries for each water quality condition (i.e., CRW/SPW blend and CRW at both pH 8.3 and 7.0). It should be noted that for certain tests, a positive change normalized flux occurred at the end of the runs (e.g., see last data points for controls in Figure 17 and Figure 20). Given the recirulatory nature of the bench-scale experiments, these increases in normalized flux were most likely attributed to effect of increasing osmotic pressure of the feed solution lowering the net driving pressure exerting a greater influence on normalized flux than the decreasing permeate flow. Membrane failure may also play a role, but salt rejection data do not support this conclusion. A more detailed discussion of the normalized flux results follows.

Figure 21 presents a summary of the relative flux declines for all antiscalants and water types. For both commercial and generic antiscalants, antiscalant performance differed when using CRW/SPW blended water as opposed to 100 percent CRW (both pH 8.2 and 7.0). For example, the antiscalants that outperformed the control in the blended water were seldom found to perform better than the control in 100 percent CRW (either pH 8.2 or pH 7.0). The difference between the blended water and the CRW waters indicated that the two types of waters were different as far as the scale forming potential was concerned, and that antiscalants performed well in one type of water might not be a good choice for the other. On the other hand, the performance of antiscalants in the pure CRW (pH 8.2) and CRW at pH 7.0 were consistent with each other, i.e., those antiscalants outperformed the control in these two types of waters were almost the same. The flux decline of the control (no antiscalant condition) in the blended water was 10 percent less than the pure CRW, which accounted for 35 percent improvement of performance relative to pure CRW. The better performance of the control in the blended water indicated that pure CRW was more prone to scaling than the blended water. pH adjustment of CRW water from pH 8.2 to 7.0 demonstrated a positive effect on flux decline as evidence by less flux decline of both the control and almost all antiscalants tested in CRW at pH 7 than in pure CRW. Another observation was that many antiscalants showed larger flux decline than the control tests,

suggesting either; (1) the bench-scale RO unit measurements lacked adequate sensitivity to distinguish between changes in flux, or (2) the 95 percent water recovery concentrated the salts such that they overwhelmed the antiscalant and the level of fouling was indistinguishable from the control.

Antiscalant CA1 outperformed all other commercial antiscalants in the blended water (see Figure 21). The flux decline for CA1 was 7 percent, while all others (including control) had at least twice (14 percent) reduction of the flux in the blended water. Actually, CA1 was the only commercial antiscalant that performed significantly better than the control in blended water. Generic chemicals GC4.2 and GC4.3 also demonstrated better performance than the control. However, GC4.2 showed significant flux increase at high water recovery and data points at water recovery higher than 85 percent for GC4.3, where usually most flux reduction occurred, were missing (see Figure 18).

Many commercial antiscalants and generic chemical showed better performance than the control in both pure CRW and CRW with pH adjusted to 7.0. These antiscalants included CA5, CA6, CA 7, CA8, GC1.4, GC3.2 and GC5.2, with antiscalant CA6 being the best in pure CRW. Besides the antiscalants listed, CA1 was also effective in CRW at pH 7.0. However, generic chemicals were less comparable than the commercial antiscalants because data on water recovery at 95 percent were usually missing for generic chemicals (see Figure 18, Figure 19, and Figure 20). The flux increases in the control test and in some commercial antiscalants may have been caused by membrane failure.

Interestingly, for any one generic chemical, higher concentration did not render better performance. Actually, different concentrations make large differences in the chemical performance, e.g., the difference of flux change was more than 50 percent between antiscalants GC1.1 and GC1.2 in blended water. Therefore, finding the optimal concentration range for an antiscalant is as important as finding the appropriate antiscalant.

Water Quality Data

Brine samples from each antiscalant trial were filtered through a 0.45 µm filter. Any solute in the filtrate (the water that passed through the filter) was considered dissolved. Each

filtrate sample was analyzed for calcium, barium, aluminum, and silica. Antiscalant effectiveness was evaluated in terms of degree of solubilization relative to a control (no antiscalant) with the theory being any ion in the dissolved phase had a lower scaling potential than ions in the non-dissolved phase. Antiscalants, if effective for a given solute, should complex with the solute and remain in the dissolved phase, i.e. no precipitation should occur.

Potential forms of calcium precipitates in CRW include calcium carbonate ($CaCO_3$), calcium sulfate ($CaSO_4$) and calcium fluoride (CaF_2). However, EDS data for all membrane samples were inconclusive for sulfate and showed no fluoride present on the membrane surface. Additionally, most samples showed strong effervescence when exposed to 0.1 *N* HCl. Therefore, the calcium precipitates present during this testing were most likely calcium carbonate.

The distribution patterns of dissolved calcium present in the filtrate of the brine samples (see Figure 22) in each of the three types of waters appeared very similar to those demonstrated in permeate flux (see Figure 21). The better performance of controls in blended water and in CRW at pH 7.0 again indicated that CRW was more prone to calcium scaling and that pH adjustment from 8.2 to 7.0 efficiently solubilized calcium. The distribution similarity between dissolved calcium and flux also demonstrated that calcium scales were the major scales in these waters.

Antiscalants that outperformed the controls usually showed less than 10 percent of the solubilization capacity. Given the excess of calcium in the system (greater than 50 mg/L), a measurable increase on calcium may not be measured via water quality analyses, despite calcium precipitation occurring. Antiscalant GC1.3 increased the dissolved calcium by 25 percent (of the total calcium in the feed) over the control in the blended water because the citric acid concentration was over 100 mg/L (see Table 10) and could easily form a water soluble complex with calcium carbonate. Antiscalant CA5 demonstrated almost 10 percent increase of dissolved calcium in both CRW (pH 8.2) and CRW at pH 7.0. This finding suggests that in addition to containing 2-propenoic acid (see Table 11), antiscalant CA5 may

contain calcium as part of its formulation. Generally speaking, commercial antiscalants performed better than generic chemicals in CRW waters.

Barium can react with sulfate to form barium sulfate ($BaSO_4$) scale—which has the highest scale forming potential in CRW (pH 8.2), see Task 1. That the dissolved barium in the control of pure CRW at 95 percent water recovery was less than 10 percent of the total barium originally present (see Figure 23) also demonstrated barium's insolubility. However, while barium was not in the dissolved form, no barium scaling was detected on the membrane surface via EDS. Actually, the relatively higher levels of barium in the control samples in blended water and CRW at pH 7.0 also indicated that the blended water was less prone to barium scaling than CRW, and that pH adjustment had the positive effect on dissolving barium—though barium sulfate scale potential has been shown to be fairly insensitive to pH adjustment (see Task 1). This is the same pattern observed in flux and in the calcium diagrams (see Figure 21 and Figure 22).

Antiscalants CA1 and CA2 showed a strong ability to bind barium in the blended water. The dissolved barium was increased by 45 percent, which was more than 2.5 times that of the control. Antiscalant CA3 significantly outperformed the experimental control in pure CRW, i.e. dissolved barium increased by 35 percent over the control. Generic chemicals generally were not as efficient as the commercial antiscalants in sequestering barium from each water type. Antiscalant GC1.3 in the blended water performed the best among the generic antiscalants by increasing the dissolved barium by 20 percent over the control. In general, generic antiscalants offered no significant improvement in barium sulfate scale formation in CRW.

Scanning Electron Microscopy and Energy Dispersive Spectroscopy Analyses of the Membrane Surface

SEM provides a visual picture of the scales forming on the RO membrane surface (qualitative analysis) while EDS presented the amount of element components in the scales on the RO membrane (both qualitative and quantitative analyses). Therefore, SEM and EDS data offered direct information on the performance of antiscalants in reducing the amount

and type of scales. Unfortunately, the EDS analysis may be biased since its sampling area is very small and big scale grains had to be avoided.

Based on visual SEM data, two types of fouling were observed (see Figure 24 and Figure 25 for representative SEM micrographs): organic fouling and inorganic fouling. Assuming that insufficient time passed to allow for biological fouling, the organic material present on the membrane surfaces were assumed to be from the antiscalant(s) precipitating out of solution at high water recovery. Organic material on the membrane surface is particularly undesirable due to organic materials being a potential food source for bacteria, as well as a potential attachment site for colloids and inorganic scales. Organic fouling was observed more often in membranes treating CRW at pH 7.0 (antiscalants CA3 through CA8) (see Table 12).

According to EDS data, inorganic scales were predominately calcium-based scales, most likely calcium carbonate. Both SEM and EDS data showed that commercial antiscalants had less scaling in the blended water than in CRW at pH 7.0 and 8.2 (see Table 12 and Table 13). Almost no scales were present on the RO membrane surface of antiscalants CA1 and CA2, indicating CA1 and CA2 were effective antiscalants for treating calcium scaling in the blended water. Commercial antiscalants were not as efficient in reducing calcium scaling in CRW at pH 8.2 as in CRW at pH 7.0 (see Table 12 and Table 13) because pH adjustment (decrease from 8.2 to 7) was useful increasing the solubility of calcium carbonate. However, organic fouling was encountered with the pH adjustment for antiscalants CA3 through CA8. On the other hand, generic chemicals generally were not good in treating the calcium scales (see Table 12), but organic fouling was not encountered.

Analysis of Colloidal Material

An analysis of the colloidal material in the concentrate was conducted by filtering brine samples through a 0.45 µm membrane. Colloidal material is experimentally defined as material that did not pass through the 0.45 µm filter. The retentate, or filter cake, from the RO concentrate was evaluated in terms of its physical characters (e.g., color, thickness, texture and permeability), elemental composition (see Table 13), and calcium carbonate content, as indicated by effervescence with 0.1 *N* HCl.

Generally speaking, filter cake performance for both commercial antiscalants and generic antiscalants was no better than the control tests in the waters tested (see Appendix D, Tables D.1 through D.4). Calcium was the major component in the cake, and silica was the minor one (see Table 13). Silica was more frequently present in the cakes of generic antiscalants than of commercial antiscalants. The generic antiscalant's inability to bind silica may have resulted in amorphous silica precipitating out of solution at very high water recovery (95 percent). The degree of calcium carbonate scaling of filter cakes were similar among the commercial and generic antiscalants, except for antiscalants GC1.2 and GC1.3 where no carbonates were observed. Both GC1.2 and GC1.3 were citric acid at relatively high concentrations (1200 mg/L and 120 mg/L, respectively) where calcium citrate complexation should take place.

Prevention of Aluminum Silicate Formation

Experiments with Ambient Aluminum

Silica and aluminum each contribute to the formation of aluminum silicates. Dissolved silica constituted a significant portion of the overall silica in the system in the three water types; dissolved silica in the controls was 63, 78, 85 percent of the total silica in the feed waters respectively (see Figure 26). Commercial antiscalants demonstrated higher affinity to bind silica than the generic chemicals. For instance, CA7 showed binding with silica in both blended water and CRW at pH 7.0. Antiscalant CA1 outperformed all other antiscalants in pure CRW. For a majority of generic chemicals, silica was found precipitated on membrane surface and in colloidal materials of the concentrate (see Table 13). Silica precipitation indicated generic chemicals were less efficient in complexing silica than commercial antiscalants.

Generic antiscalants were selected for control of aluminum silicate precipitation based on their ability to complex with aluminum. Thus, the generic chemicals were more efficient in binding aluminum than commercial antiscalants in the blended water (see Figure 27). Antiscalant GC1.2 and GC1.3 increased the dissolved percentage of aluminum by 50 percent, which amounted to over 200 percent improvement of binding efficiency relative to the

control in the blended water. Antiscalant GC5.1 and GC5.2 also increased the efficiency of aluminum binding by 100 percent relative to the control in the blended water. Therefore, citric acid and EDTA appeared to be better aluminum complexation agents than other commercial and generic antiscalants. These generic antiscalants, which were originally proposed for treating aluminum silicate scales in Task 2, were proven effective silicate inhibitors by complexing aluminum into a soluble form that would otherwise be used to form aluminum silicates. Therefore, silica was freed from the formation of silicate, and deposited as amorphous silica (see Table 13).

Antiscalant CA6 increased the dissolved aluminum by 140 percent in the blended water the total dissolved aluminum exceeded 100 percent, indicating sample contamination had occurred. Antiscalant CA2 also demonstrated 40 percent dissolved aluminum increase in the blended water. Antiscalants CA7 and GC1.4 slightly increased the dissolved aluminum in CRW at pH 8.2. No commercial and generic antiscalants showed a strong ability to bind with aluminum in CRW at pH 7.0. pH adjustment (from 8.2 to 7.0) considerably decreased the solubility of aluminum in CRW (see levels of controls in Figure 27). This agrees with aluminum solubility theory and that aluminum ion (Al^{3+}, at pH 7) regulated the formation of aluminum silicate scales in CRW.

Experiments with Added Aluminum

During the conventional treatment process at Metropolitan's drinking water plants, aluminum sulfate (alum) coagulation is often employed. Based on dosage rates and aluminum's inherent solubility, approximately 200 µg/L of aluminum is commonly measured at the filter effluent. This effluent would theoretically serve as the feed to any desalting step. Therefore, in order to mimic this water quality condition, excess aluminum (as $Al(NO_3)_3 \cdot 9H_2O$) was added to the microfiltered source water to yield 200 µg/L dissolved aluminum. In addition, the pH of the feed water was reduced to pH 6.7 to avoid calcium carbonate scaling, which may complicate data interpretation. The measured aluminum in the source water was 170 µg/L, which agreed closely with the theoretical yield. Therefore, prior to RO treatment a majority of the aluminum remained in solution.

When the amount of aluminum was insufficient, aluminum silicates were not formed as shown in the tests of commercial antiscalants and generic antiscalants described above. Therefore, silicate scale inhibition may be achieved by removing aluminum in CRW. Modeling results from Task 2 also showed that the total dissolved aluminum was 99 percent in the form of $Al(OH)_4^-$ at pH 8.2. Because $Al(OH)_4^-$ at pH 8.2 would be converted to Al^{3+} at pH 7.0, Al^{3+} was the sole important ion in aluminum silicate formation in CRW both predicted by modeling and in the aluminum addition tests. Thus, the strategy of minimizing silicate scaling by complexing aluminum may be promising. Also, results of scale potential of aluminum above had shown that all generic antiscalants were efficient in binding aluminum.

As a result of aluminum addition in the form of $Al(NO_3)_3 \cdot 9H_2O$, both aluminum and silica were detected by EDS in the filter cake for the control (see Table 14) indicating the formation of aluminum silicates. Furthermore, most filter cakes contained gray-colored material that cracked upon drying, which was a typical character of clay-containing scales found previously at Metropolitan (Gabelich et al. 2000). When the gray precipitate was exposed to 0.1 *N* HCl, the material did not dissolve and minimal, if any, effervescence was observed indicated a lack of calcium carbonate scaling. Additionally, the acid test provided a key indication that the gray precipitate material was aluminum silicate, rather than aluminum hydroxide in nature. Below pH 5.7, freshly precipitated aluminum hydroxides are quite soluble (Faust and Aly 1998). These results demonstrated that aluminum played a vital role in the formation of aluminum silicate scales in CRW.

Combinations of a commercial antiscalant (CA1) and two generic antiscalants (citrate [GC6] and EDTA [GC5.3]) were used in this test. Note: citrate and citric acid are essentially the same chemical, only the counterion differs between the two. Since CA1 had demonstrated its ability to remove calcium and barium scales and generic antiscalants GC5.3 and GC6 were good at sequestering aluminum, combinations of these antiscalants may provide protection against both traditional (e.g., barium sulfate and calcium carbonate) and non-traditional (i.e., aluminum silicates) scales.

Specific flux data for each of the six RO runs using excess aluminum showed little variation despite permeate flows decreasing by as much as 66 percent (see Figure 28), most likely due to operational limitations describe previously. In terms of solubilization, citrate (GC6) showed the greatest ability to keep aluminum in the dissolved phase, while EDTA (GC5.3) showed the greatest ability to solubilize silica (see Figure 29). Adding a commercial antiscalant (CA1) did not improve the aluminum binding potential for either GC6 or GC5.3, though no aluminum was found in the colloidal phase, as well (see Table 14). These data may indicate that for antiscalant CA1, a majority of the aluminum was deposited on the membrane surface (further discussion to follow). The silica data for two of the experiments (CA1, and CA1/GC6) are unavailable, though previous testing using both CA1 and GC6 showed no effect on silica solubility (see Figure 26).

SEM data showed a clay-like coating on the membrane surfaces for most experiments using excess aluminum (see Figure 30). Notable exceptions are experiments using GC6 and GC5.3, which show white grains on the membrane surface with little other foulants present. These grains may be calcium carbonate or calcium sulfate scales being that no protection against these foulants (i.e., a commercial antiscalant) was present. EDS data indicated the presence of calcium for the GC5.3 sample (see Table 15); the EDS method uses a small sample area and may not include the grains in the analysis. Therefore calcium may have been present in the GC6 sample, but not detected.

Aluminum was detected by EDS for all samples, with the exception of the GC6 sample. For this sample, the visual evidence supports the lack of aluminum silicate fouling (Figure 30) based on the absence of semi-porous clay-like material on the membrane surface. In addition, generic antiscalant GC6 demonstrated superior performance in keeping aluminum in solution (see Figure 29) that may have prevented aluminum from precipitating as either a silicate or hydroxide material. While no visual evidence of aluminum silicate were observed on the GC5.3 sample, EDS data detected the presence of both aluminum and silica on the membrane surface. Therefore, both GC6 and GC5.3 demonstrated good aluminum silicate preventative properties, GC6 more so than GC5.3.

The combination of GC6 and CA1 showed the strong presence of aluminum and silica on the membrane surface (see Table 15) despite this combination's ability to keep aluminum in the soluble form (see Figure 29). The CA1/GC5.3 combination also showed presence of aluminum in excess of the generic antiscalant alone, but no silica was detected (Table 15). These data may suggest that the commercial antiscalant component of the mixture may have reacted with the aluminum to form a precipitate. Phosphorous, a key inorganic component of the CA1 antiscalant, was detected in the colloidal phase for both antiscalant combination experiments (see Table 14), which may support the theory that the aluminum reacted with the commercial antiscalant. However, given the ability of antiscalant GC5.3 to sequester silica (see Figure 29), the precipitate may be in the form of an aluminum hydroxide, which is supported by the lack of silica detected on the membrane surface (see Table 15). In addition, both silica and aluminum were detected in the CA1/GC6 sample, indicating fouling due to aluminum silicates and/or aluminum hydroxides. These precipitates may be in the form of aluminum silicates or aluminum hydroxides. A potential fouling pathway is through the creation of an aluminum hydroxide or other bound-aluminum foulant that originally precipitates onto the membrane surface, and then these foulants serve as nucleation sites for aluminum silicate formation.

Based on the limited experimental data, citrate and EDTA may effectively act as aluminum sequestering agents that may lead to the prevention of aluminum silicate or hydroxide scaling. However, the commercial antiscalant itself may act as a catalyst or intermediary for aluminum-based scalant formation.

Overall Performance of Antiscalants

Permeate flux decline is the only parameter demonstrating the overall performance of an antiscalant. Permeate flux results showed that antiscalant CA1 excelled other antiscalants in the blended water; antiscalant CA6 was the best in CRW at pH 8.2, and the difference in antiscalant performance in CRW at pH 7.0 was less distinguishable.

Unfortunately, analyses performed in the three locations of the RO process were not directly comparable with each other because some data were quantitative (e.g., water quality data),

others were qualitative (e.g., SEM data and visual description of the colloidal material) and still others were semiquantitative (e.g., EDS data). Also, each set of data described one aspect of the antiscalant performance and each should not be weighted equally in its importance. Antiscalant performance on the formation of precipitation on the membrane surface should weigh heavier than data about the concentrate (in forms of dissolved or colloidal phase) because what was in the concentrate only had a potential to form scales. When scales were not formed, dissolved element data (water quality data) should develop a more accurate description of the antiscalant performance since these data were quantitative. Under such a guideline, antiscalants CA1 and CA2 performed better than other antiscalants in the blended water. Therefore, the commercial antiscalant CA1 (Permacare, Permatreat 191) was selected for the pilot-scale testing. No antiscalant showed a significant better overall performance than other antiscalants in CRW (pH 8.2 and 7.0). Antiscalant CA6 could be used for treating CRW at pH 8.2.

Generic chemicals, especially citric acid and EDTA, demonstrated strong ability to treat the non-traditional scales (i.e. aluminum silicates) by complexing with aluminum. Adding a commercial antiscalant (Permacare, Pretreat 191) did not improve the generic chemicals ability to control for aluminum silicate fouling, and may be a contributing factor in aluminum-based scalant formation.

CONCLUSIONS AND RECOMMENDATIONS

General Conclusions

Pilot-Scale Evaluation of Reverse Osmosis and Nanofiltration Membranes

Of the five RO membranes evaluated during this study, RO1 (Dow Separation Processes, FilmTec LE) provided the highest specific flux (0.37 gfd/psi) while still maintaining high salt rejection (98.8 percent). Performance data for NF membranes provided a wider range of variation in water production and salt rejection properties than RO membranes. While NF membranes generally provided high specific flux and lower salt rejection than the RO membranes tested, membrane NF1 (Dow Separation Processes, FilmTec NF90) showed comparable specific flux and salt rejection (0.36 gfd/psi and 98.6 percent, respectively) to

that of RO1. However, the ultimate selection of an appropriate membrane is predicated on the specific application's water quality and quantity goals.

Ion hydrated radius and solution pH had a direct impact on the salt rejection behavior of NF membranes. Generally, as the hydrated radius increased (e.g., from sodium to sulfate), the rejection of that ion also increased. Additionally, operation at low pH conditions increased NF membrane salt rejection through chemically tightening of the membrane surface.

Economic Evaluation of Reverse Osmosis and Nanofiltration Membranes

Each of the four experimental RO membranes studied (RO1, RO3, RO4, and RO5) improved overall membrane systems costs by at least 15 percent. Therefore, the project goal to reduce the membrane system cost by 10 percent was met. Of the RO membranes tested, RO1 demonstrated the highest specific flux (0.37 gfd/psi) while still maintaining excellent salt rejection (98.8 percent) (see Table 9). These two factors resulted in RO1 showing the greatest cost savings (20 percent) over current commercial RO membranes. Two of the NF membranes tested (NF1 and NF7) demonstrated superior performance in terms of both specific flux and salt rejection over a current commercially available ultra-low-pressure RO membrane, resulting in a 19 and 14 percent cost savings, respectively. Therefore in order to minimize the capital and O&M costs for a membrane system, membrane selection plays a vital role.

Evaluation of Commercial and Generic Antiscalants

The primary scalants of concern were calcium carbonate and barium sulfate. The degree of scaling from these constituents was predicated on source water quality and the water recovery. Selection of the appropriate antiscalant is predicated on influent water quality, pretreatment type, and system water recovery.

For Colorado River water, phosphonate-based antiscalants performed well at 85 percent water recovery. A potential mitigation strategy for aluminum silicate scale formation is through the use of complexing agents to bind with the dissolved aluminum. Potential aluminum complexing agents include citric acid and EDTA. Bench-scale experiments confirmed that both citric acid and EDTA might be effective in preventing the aluminum

silicate scales. However, when both citrate (chemically similar to citric acid) and EDTA were used in tandem with a phosphonate-based antiscalant, aluminum silicate fouling was observed. The phosphate component of the commercial antiscalant may have reacted with the dissolved aluminum to form an aluminum phosphate foulant, which may serve as an intermediate step towards aluminum silicate fouling.

Commercialization Potential

To ensure commercial viability and the implementation of newly developed technology, project results will be published in refereed journals and presented at national conferences to water and wastewater industry professionals. The purpose of publications/presentations is to disseminate technical information to a broad range of industry representatives. Results for this study can then be incorporated into ongoing research and development activities throughout California, and the country. In addition, suppliers of membrane and membrane-related technologies will develop comparable products to maintain competitiveness in the industry.

Recommendations

With the development of polyamide membranes, not only has the operating pressures for membrane systems decreased, but the water production per psi has also increased substantially. However, future increases in energy savings will not be as dramatic due to the approaching physiochemical limits for driving pressure. Currently, NF membranes operate at significantly higher flux rates than RO membranes, but exhibit poorer salt rejection. Further research is needed to combine the high water production of NF membranes with the high salt rejection of RO membranes. Additional research is needed to develop next generation membranes such that they are either chlorine tolerant to prevent biofouling or exhibit unique surface charge characteristics that prevent particle and bacterial adhesion, or even scaling.

This project only evaluated a small fraction of the total number of antiscalant types available for municipal water treatment. In order to facilitate information exchange between research groups, a standardized antiscalant test protocol needs to be developed. A primary concern

with antiscalant testing is achieving representative water quality conditions that mimic those found in full-scale treatment plants at a given water recovery. Closed-loop membrane testing, while inexpensive, may not provide representative water quality conditions and single-pass, multi-array membrane systems are not only expensive but have high water flow rate demands (up to 20 gpm). Therefore, smaller, single-pass membrane test systems need to be developed. Additionally, a standardized protocol for interpreting RO membrane and water quality data to judge antiscalant effectiveness needs to be developed.

Benefits to California

This project, entitled *Electrotechnology Applications for Potable Water Production and Protection of the Environment*, was an integrated part of a larger program; the Desalination Research and Innovation Partnership (DRIP). The overall goal of the DRIP program is the cost-effective demineralization of CRW, as well as other water sources. Results from this study, as well as other interrelated studies, will enable local municipalities to adopt desalination technologies to treat current and previously unusable potable water supplies.

The primary economic benefit of the DRIP program is the reduction of societal damages to the public and private sectors due to high salinity of Colorado River water. An additional benefit is the reduction of energy usage to reduce the TDS of CRW over currently available technologies. These are broad societal, or public interest, benefits that conform to PIER goals. Each acre-foot of CRW treated by technologies derived from this project would require less energy than current desalination practices, or through importing low salinity water from Northern California. Additionally, technologies evaluated during this project may be applicable to other source waters in California, including municipal wastewater, brackish groundwater, and agricultural drainage water.

REFERENCES

Anselme, C., and Jacobs, E.P. 1996. Ultrafiltration. In *Water Treatment Membrane Processes.* Edited by J. Mallevialle, P.E. Odendaal, and M.R. Wiesner. New York: McGraw-Hill.

Atkins, P. and L. Jones. 1997. Reverse Osmosis. In *Chemistry: Molecules, Matter, and Change*. New York: W.H. Freeman and Co.

Bersillon, J.-L.; & Thompson, M. A. Field Evaluation and Piloting. In *Water Treatment: Membrane Processes* (Ed. J. Mallevialle, P. E. Odendaal, M. R. Wiesner). McGraw-Hill, New York, 1996.

Boffardi, B. P. Scale Deposit Control for Reverse Osmosis Systems. Calgon Corporation Technical Paper, Bulletin No. 4-165, 1996

Colorado River Basin Salinity Control Forum. Water Quality Standards for Salinity. Colorado River System, 1996.

Darton, E. G. Scale Inhibition Techniques Used in Membrane Systems. *Desalination* Vol. 113, 227-229, 1997.

Geraldes, V.M., C.A. Semiao, and M.N. de Pinho. 1998. Nanofiltration Mass Transfer at the Entrance Region of a Silt Laminar Flow. *J. Industrial and Engineering Chemistry Research*, 37(12):4792-4800.

Jacangelo, J.G. 1999. *Membrane Filtration for Small Drinking Water Systems.* Online: Environmental Protection Agency. http://www.epa.gov/rgytgrnj/programs/wwpd/workshop99/membrane.pdf.

Jacangelo, J.G., and C.A. Buckley. 1996. Microfiltration. In *Water Treatment Membrane Processes.* Edited by J. Mallevialle, P.E. Odendaal, and M.R. Wiesner. New York: McGraw-Hill.

Nightingale, E.R. Jr. 1959. Phenomenological Theory of Ion Solvation: Effective Radii of Hydrated Ions. *J. Phys. Chem.*, 63(9):1381-1387.

NSF International (National Sanitation Foundation International). 2000. EPA/NSF ETV Equipment Verification Testing Plan for the Removal of Inorganic Chemical Contaminants by Reverse Osmosis or Nanofiltration. *EPA/NSF ETV Protocol for Equipment Verification Testing of Removal of Inorganic Constituents.* Ann Arbor, Mi.: NSF International.

Paulson, D. and K. Jondahl. 1999. Crossflow Membrane Filtration. In *Application of Membrane Technology for the Recovery and Reuse of Water*. Online: Osmonics. http://www.osmonics.com/products/Page771.htm

PTI Advanced Filtration Inc. (Purification Through Innovation). 1999. *Industrial Membrane Separation Process Technology*. Online: PTI Advanced Filtration Inc. http://www.pti-afi.com/technology.htm.

Taylor, J. and E. Jacobs. 1996. Reverse Osmosis and Nanofiltration. In *Water Treatment Membrane Processes.* Edited by J. Mallevialle, P.E. Odendaal, and M.R. Wiesner. New York: McGraw-Hill.

Wiesner, M.R. and P. Aptel. 1996. Mass Transport and Permeate Flux and Fouling in Pressure-Driven Processes. In *Water Treatment Membrane Processes.* Edited by J. Mallevialle, P.E. Odendaal, and M.R. Wiesner. New York: McGraw-Hill.

Wiesner, M.R. and C.A Buckley. 1996. Principles of Rejection in Pressure-Driven Membrane Processes. In *Water Treatment Membrane Processes.* Edited by J. Mallevialle, P.E. Odendaal, and M.R. Wiesner. New York: McGraw-Hill.

GLOSSARY

Colorado River water - influent water source from Lake Mathews, California, the southern terminus for the Colorado River aqueduct system.

Energy dispersive spectroscopy (EDS) - A group of techniques used to analyze the atomic structure of materials. In laboratory instruments, dispersion of radiation often occurs by the use of a prism or diffraction grating. Normal dispersion occurs when the change in refractive index increases with increasing frequency (decreasing wavelength). When the reverse occurs, absorption takes place. The absorption of radiation by materials serves as the basis for a number of types of spectroscopic analyses.

Flux - The volume or mass of permeate passing through the membrane per unit area per unit time.

Fouling - The deposition of material such as colloidal matter, microorganisms, and metal oxides on the membrane surface or in its pores, causing a decrease in membrane performance.

Langelier saturation index (LSI) - Calcium carbonate saturation index computed by the difference between the measured pH and the pH at saturation with calcium carbonate.

Microfiltration (MF) - A pressure driven membrane process that separates particles as small as 0.1-micrometer-diamter from a feed stream by filtration. The smallest particle size removed is dependent of the pore size rating of the membrane.

Natural organic matter (NOM) - A heterogeneous mixture of organic matter that occurs ubiquitously in both surface water and groundwater, although its magnitude and character differ from source to source.

Normalized flux - The permeate flow rate through the membrane adjusted to constant operating conditions.

Not detected (ND) - Compounds not detected in samples analyzed

Not sampled (NS) - A sample was not collected to be analyzed.

Rejection - In a pressure-driven membrane process, a measure of the membrane's ability to retard or prevent passage of solutes and other contaminants through the membrane barrier.

Reverse osmosis (RO) - A pressure-driven membrane separation process that removes ions, salts, and other dissolved solids and nonvolatile organics. The separation capability of the process is controlled by the diffusion rate of solutes through the membrane barrier and by sieving. In potable water treatment, reverse osmosis is typically used for desalting, specific ion removal, and natural and synthetic organics removal.

Scale - Coating or precipitate deposited on surfaces.

Scanning electron microscopy (SEM) – Electron microscope techniques where an electron beam operates as a probe by being deflected across the surface of a specimen coated with gold and palladium.

Specific flux - The permeate (water) flux divided by the net driving pressure.

State Project water (SPW) - influent water source from Northern California via the California State Water Project.

Trans-membrane pressure (TMP) - The net pressure loss across the membrane. For microfiltration and ultrafiltration with negligible osmotic pressure differential across the membrane, the hydraulic pressure differential from feed side to permeate side.

Total dissolved solids (TDS) - The weight per unit volume of solids remaining after a sample has been filtered to remove suspended and colloidal solids.

Total organic carbon (TOC) - A measure of the concentration of organic carbon in water, determined by oxidation of the organic matter into carbon dioxide. Total organic carbon includes all the carbon atoms covalently bonded in organic molecules.

TABLES AND FIGURES

Table 1. Basic properties of membrane processes

Attributes	Pretreatment		Final Treatment	
	Microfiltration	Ultrafiltration	Nanofiltration	Reverse Osmosis
Particle Size Exclusion	~0.1 μm	~0.01 μm	~0.001 μm	~0.0001 μm
Primary Use	Particles, bacteria, and some viruses	Particles, bacteria, and viruses	TDS, bacteria, and virus	TDS, bacteria, and virus
Typical Operating Pressures	10-25 psi	25-150 psi	70-250 psi	125-1000 psi

Adapted from Jacangelo 1999

Table 2. List of commercial test membranes

Code	Manufacturer	Membrane	Membrane Type
Reverse Osmosis Membranes			
RO1	Dow Separation Processes	FilmTec Enhanced LE	Ultra-low-pressure
RO2	Koch Fluid Systems	TFC-ULP®	Ultra-low-pressure
RO3	Hydranautics	LFC1	Low-fouling composite
RO4	Hydranautics	ESPA3	Ultra-low-pressure
RO5	Hydranautics	ESPA1	Ultra-low-pressure
Nanofiltration Membranes			
NF1	Dow Separation Processes	FilmTec NF90	Ultra-low pressure
NF2	Dow Separation Processes	FilmTec NF200	Ultra-low pressure
NF3	Hydranautics	Prototype CTC50	Chlorine tolerant composite
NF4	Koch Fluid Systems	SR1	Ultra-low pressure
NF5	Koch Fluid Systems	SR2	Ultra-low pressure
NF6	TriSep	TS80-TSA	Ultra-low pressure
NF7	TriSep	XN40-TZF	Ultra-low pressure

Table 3. Nanofiltration membrane test matrix

Membrane	pH	Percent Recovery
NF1	8.1	10, 50, 85
NF2	8.1	10, 50, 85
	6.5	10, 50, 85, 90
	4.8	10, 85
NF3	8.1	10, 50, 85
	6.5	10, 50, 85, 90
	4.8	10, 85
NF4	8.1	10, 85
NF5	8.1	10, 85
NF6	8.1	10, 90
NF7	8.1	10, 90
		Total Number of Tests: 29

Table 4. Commercial and generic antiscalant test matrix

		Dosage (mg/L)		
Vendor	Antiscalant	CRW/SPW	CRW (pH 8.2)	CRW (pH 7.0)
Permacare	PermaTreat 191	1.6	1.6	1.6
BFGoodrich	AF 1025	2.5	2.5	2.5
KingLee	RO-C and RO-D	10 (each)	10 (each)	10 (each)
BFGoodrich	AF 1405	2.5	2.5	2.5
Stockhausen	90378	10 mg/L	10 mg/L	10
Calgon	EL5300	5	5	5
BetzDearborn	Hypersperse SI300 UL	2.3	2.3	2.3
PWT	SpectraGuard	10	10	10
Generic	Citric acid	0.002	0.002	0.002
		1.1	1.1	1.1
		0.11	0.11	0.11
		0.01	0.01	0.01
Generic	Oxalic acid	0.0014	NS	0.008
Generic	Aspartic acid	0.002	0.011	0.011
Generic	Salicylic acid	0.12	NS	NS
		0.012	NS	NS
		0.002	NS	NS
Generic	EDTA	0.13	NS	NS
		0.013	0.013	0.013

NS =Not sampled

Table 5. Summary of Membrane Performance

Code	Normalized Flux (gfd)*	Specific Flux (gfd/psi)	Nominal Salt Rejection (percent)†
Reverse Osmosis Membranes‡			
RO1	20.5	0.37	98.8
RO2	16.4	0.22	93.9
RO3	12.2	0.20	98.6
RO4	18.7	0.26	99.1
RO5§	14.5	0.21	99.0
*Nanofiltration Membranes***			
NF1	23.2	0.36	98.6
NF2	18.0	0.24	82.3
NF3	24.7	0.44	54.5
NF4	24.5	0.30	64.5
NF5	25.6	0.63	52.5
NF6	21.8	0.28	62.6
NF7	18.8	0.24	97.8

* Normalized to temperature = 25ºC
† As measured by conductivity
‡ Pretreated using conventional treatment with alum
§ Pretreated using conventional treatment with ferric chloride
** Pretreated using microfiltration

Table 6. Salinity removal of nanofiltration membranes*

	Rejection (%)						
Parameter	NF1	NF2	NF3	NF4	NF5	NF6	NF7
Alkalinity	97	85	41	22	53	41	96
Total Hardness	>99	91	NS	76	90	NS	NS
Total Dissolved Solids	>99	85	61	63	72	73	99
Calcium	>99	94	69	NS	NS	NS	NS
Magnesium	>99	95	68	NS	NS	NS	NS
Potassium	>99	74	42	NS	NS	NS	NS
Sodium	>99	74	41	NS	NS	NS	NS
Silica	>99	44	3	5	14	17	95
Chloride	98	62	1	0	15	9	96
Sulfate	98	98	96	>99	99	97	99
Fluoride	95	61	40	27	56	52	95
Barium	>99	94	71	74	90	83	>99
Aluminum	96	>99	93	93	98	95	98
Strontium	>99	94	70	75	91	83	>99
TOC	93	93	19	82	86	93	97
Ultra Violet	89	85	79	85	94	94	98

* As measured by APHA, AWWA, and WEF 1998
NS = Not sampled.
Note: 10 percent water recovery, pH 8.1

Table 7. Ionic and hydrated radii of common ions found in natural waters

Ion	Ionic Radius (ångström)	Hydrated Radius (ångström)
Aluminum	0.50	4.75
Magnesium	0.65	4.28
Iron	0.75	4.28
Sodium	0.95	3.58
Calcium	0.99	4.12
Potassium	1.33	3.31
Barium	1.35	4.04
Fluoride	1.36	3.52
Chloride	1.81	3.32
Sulfate	2.90	3.79

Adapted from Nightingale 1959

Table 8. Qualitative effect of membrane productivity and salt rejection on system cost

	Δ Membrane Performance	Δ O&M Costs	Δ Capital Costs
Specific Flux	**?**	**?**	**-**
	?	**?**	**-**
Salt Rejection	**?**	**-**	**?**
	?	**-**	**?**

- = no significant change

Table 9. Economic evaluation of experimental membranes for a 300-mgd, split-flow-desalting plant to meet 500 mg/L TDS finished water quality goal

	Operational Data		O&M Costs			Capital Costs		Total Plant Costs	
Membrane	Specific Flux (gfd/psi)	Salt Rejection (percent)*	Feed Pressure (psi) †	Energy Cost ($M/yr)‡	Total O&M ($M/yr)	Membrane Plant Size (mgd) ††	Total Capital ($M/yr)	Total Membrane Plant Cost ($M/yr)	Percent Difference from Baseline
RO1	0.37	98.8	120	$2.86	$12.1	102.0	$7.56	19.6	-20
RO2§	**0.22**	**93.9**	**158**	**$4.49**	**$15.5**	**121.5**	**$9.00**	**24.5**	**0**
RO3	0.20	98.6	171	$4.08	$13.3	102.0	$7.56	20.9	-15
RO4	0.26	99.1	146	$3.45	$12.6	101.3	$7.51	20.1	-18
RO5	0.21	99.0	134	$3.17	$12.3	101.3	$7.51	19.8	-19
NF1	0.36	98.6	122	$2.92	$12.2	102.5	$7.60	19.8	-19
NF2	0.24	82.3	145	$6.42	$23.6	190.0	$14.1	37.7	+54
NF3**	0.44	54.5	97	$6.79	$33.9	300.0	$22.2	56.1	+129
NF4**	0.30	64.5	122	$8.54	$35.7	300.0	$22.2	57.9	+136
NF5**	0.63	52.5	81	$5.71	$32.8	300.0	$22.2	55.0	+124
NF6**	0.28	62.6	127	$8.90	$36.0	300.0	$22.2	58.2	+138
NF7	0.24	97.8	152	$3.74	$13.2	105.2	$7.80	21.0	-14

* As measured by conductivity

† 64°F (17.8°C) average feed temperature

‡ Assumes $0.06/kWh and 80 percent pump efficiency

§ RO2 is a commercially available ultra-low-pressure RO membrane that served as the baseline condition

** Membrane plant could not meet 500 mg/L TDS finished water quality goal

†† Membrane plant size based on 85 percent water recovery

Table 10. Reference guide for bench-scale antiscalant testing

Code	Vendor	Antiscalant	Dose (mg/L)
CA1	Permacare	PermaTreat 191	1.6
CA2	BFGoodrich	AF 1025	2.5
CA3	KingLee	RO-C and RO-D	10 (each)
CA4	BFGoodrich	AF 1405	2.5
CA5	Stockhausen	90378	10
CA6	Calgon	EL5300	5.0
CA7	Argo (BetzDearborn)	Hypersperse SI300 UL	2.3
CA8	PWT	SpectraGuard	10
GC1.1	Generic	Citric acid	2.0
GC1.2			1,200
GC1.3			120
GC1.4			12
GC1.5			24
GC2.1	Generic	Oxalic acid	2.0
GC2.2			10
GC3.1	Generic	Aspartic acid	2.0
GC3.2			11
GC4.1	Generic	Salicylic acid	117
GC4.2			12
GC4.3			2.4
GC5.1	Generic	EDTA in form of sodium salt	124
GC5.2			12
GC5.3			16
GC6	Generic	Sodium Citrate	34

Table 11. Chemical and physical information for commercial antiscalants used in bench-scale testing.

Code	Chemical and Physical Information
CA1	NA Specific Gravity (SG) 1.36 at 20°C
CA2	Water 63% Polymer/Solids 37% SG 1.15
CA3	Pretreat Plus-2000 SG 1.04 Protec RO-C and RO-D SG 1.01
CA4	Water < 71% Polymer/Solids 29% SG 1.12
CA5	2-Propenoic acid, polymer with a-(2-methyl-1-oxo-2-propenyl)-w-methoxypoly (oxy-1,2-ethanedily) and sodium 2-methyl-2-propene-1-sulfonate, sodium salt
CA6	Sodium salt of Phosphonomethylated diamine
CA7	NA SG 1.142 @ 21°C
CA8	Water soluble polymer SG 1.04-1.08

NA = not available.

Table 12. SEM results of fouled membrane surface of bench scale testing

Test	CRW/SPW blend	100% CRW at pH 8.2	100% CRW at pH 7
Control	3	4	3
CA1	1	4	3
CA2	1	OF	2
CA3	4	4	OF
CA4	2	3	OF
CA5	OF	4	OF
CA6	2	3	OF
CA7	OF	4	OF
CA8	OF	OF	OF
GC1.1	3		
GC1.2	2		
GC1.3	4		
GC1.4	5	5	3
GC2.1	5		
GC2.2			5
GC3.1	OF		
GC3.2		5	5
GC4.1	4		
GC4.2	4		
GC4.3	5		
GC5.1	5		
GC5.2	5	5	4

1 = least fouling; 2 = slight fouling; 3 = moderate fouling; 4 = severe fouling; 5 = very severe fouling; OF = organic fouling; and blank = no test.

Table 13. EDS results from membrane and colloidal analysis of bench scale testing (Data is for calcium, silica (Si) and barium (Ba) are indicated in case of presence.)

Test	Membrane Analysis			Colloidal Analysis		
	CRW/SPW blend	100% CRW at pH 8.2	100% CRW at pH 7	CRW/SPW blend	100% CRW at pH 8.2	100% CRW at pH 7
Control	2	5	2	4	4	4.5, Si=1
CA1		5	2	4	4	4
CA2		3	1	4	4.5	4
CA3	3	3.5	1	4	3.5	4.5
CA4		4	2	3.5	4	4
CA5	2	3.5	2	3.5	3.5	4.5, Si=1
CA6	2	3.5	3	3.5	3.5	4.5, Si=1
CA7	2	4	1	3.5	4	4.5, Si=1
CA8	3.5	4	1	4	4	4, Si=1
GC1.1	2, Si=1			4		
GC1.2				1, Si=2, Ba=3		
GC1.3				2, Si=2		
GC1.4	4, Si=1	3.5	2	4, Si=1	4	3.5
GC2.1	4, Si=1			4		
GC2.2			3			4
GC3.1	2, Si=1			3.5, Si=1		
GC3.2		3.5	3		3.5, Si=1	3.5, Si=1
GC4.1	3, Si=1			3.5, Si=1		
GC4.2	4, Si=1			4, Si=2		
GC4.3	2, Si=1			4,Si=1		
GC5.1	3			4, Si=1		
GC5.2	4	3.5	3	3.5, Si=2	4	4

1 = lowest; 2 = low; 3 = medium; 4 = high; 5 = highest; ND = not detectable; and blank = no test.

Table 14. EDS data of colloidal material from brine stream using CRW and 170 µg/L aluminum*

Element	Antiscalant					
	Control	CA1	GC5.3	GC6	CA1/GC5.3	CA1/GC6
Aluminum	21	--	--	16	26	19
Arsenic	--	--	--	--	--	--
Bromine	--	4.5	--	--	--	--
Calcium	12	82	94	16	17	44
Chlorine	2.8	--	--	2.0	3.1	3.1
Copper	14	4.3	--	--	--	--
Iron	--	--	--	3.3	2.3	--
Magnesium	4.2	--	1.1	6.4	4.7	4.1
Phosphorus	--	--	--	6.3	12	4.9
Potassium	--	--	--	2.3	--	--
Silica	41	6.7	--	36	24	16
Sodium	--	--	1.0	6.7	4.5	4.3
Sulfur	4.4	2.8	3.5	5.3	6.0	5.4

*Percent by weight
-- = Not detected

Table 15. EDS data from RO membranes using CRW and 170 µg/L aluminum*

Element	Antiscalant					
	Control	CA1	GC5.3	GC6	CA1/GC5.3	CA1/GC6
Aluminum	19	19	18	--	25	26
Arsenic	--	--	--	--	--	14
Calcium	--	4.3	30	--	--	--
Chlorine	--	6.4	--	8.9	--	7.3
Magnesium	--	8.1	5.3	--	--	--
Silica	10	5.6	6.9	6.8	--	5.5
Sodium	23	21	8.4	31	19	22
Sulfur	48	35	32	53	56	27

*Percent by weight
-- = Not detected

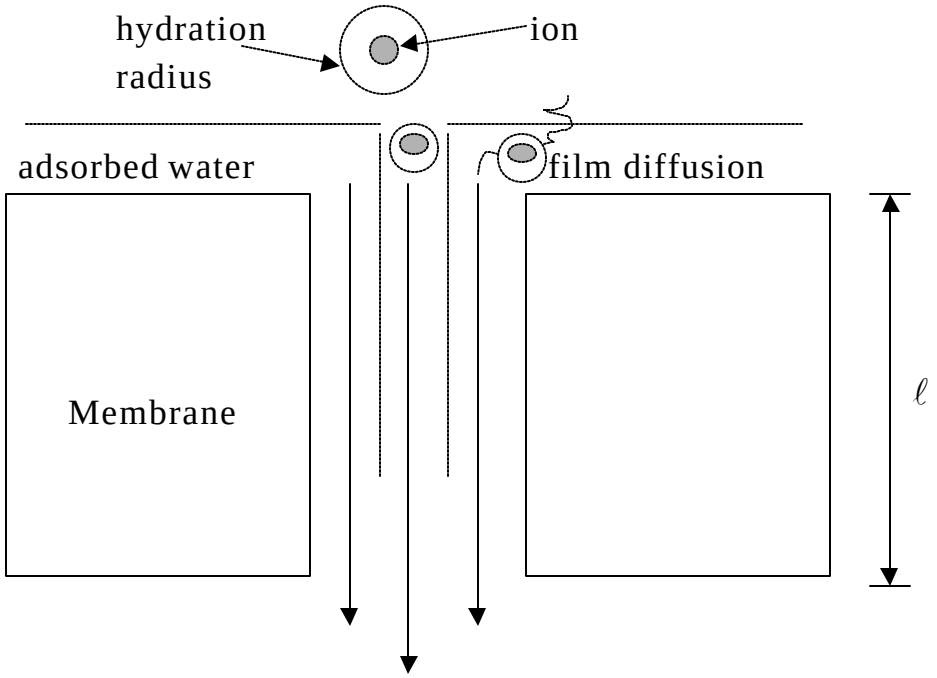

Adapted from Wiesner and Aptel 1996

Figure 1. Qualitative concept of high-pressure membrane separation processes

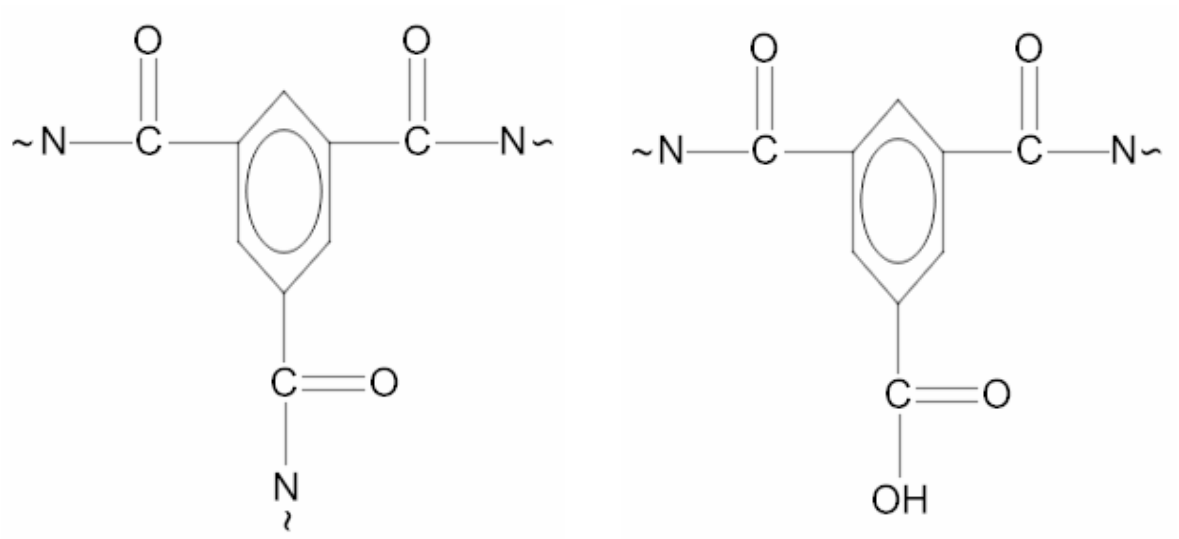

(a) (b)

Figure 2. Polymer structure of polyamide membranes: (a) reverse osmosis and (b) nanofiltration

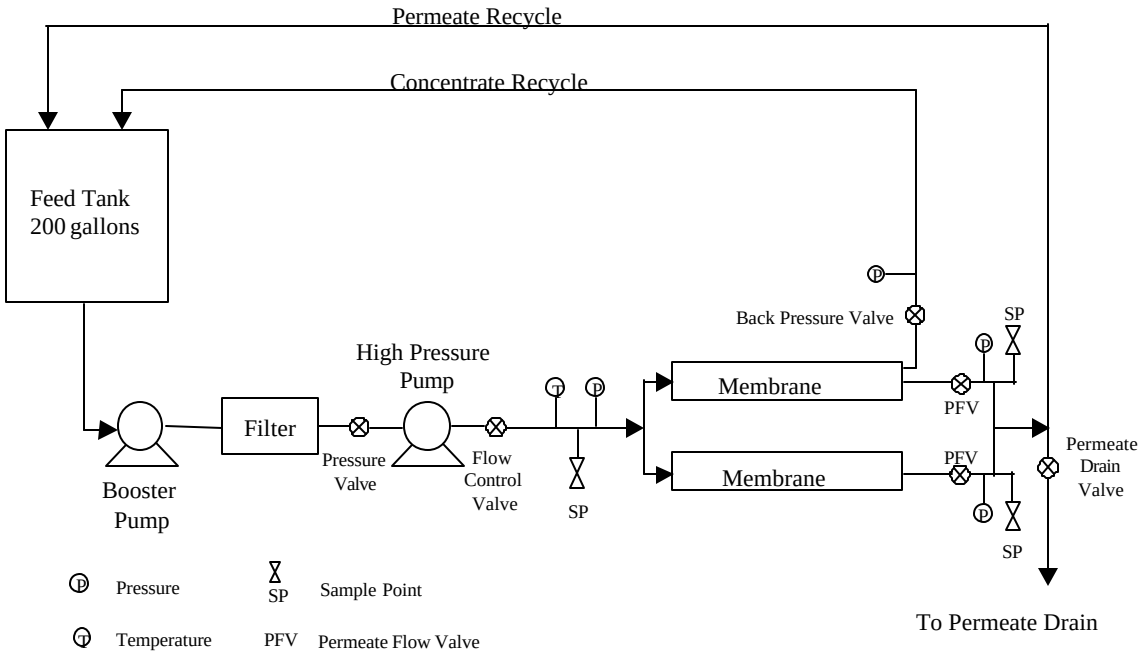

Figure 3. Schematic drawing of pilot-scale membrane test unit

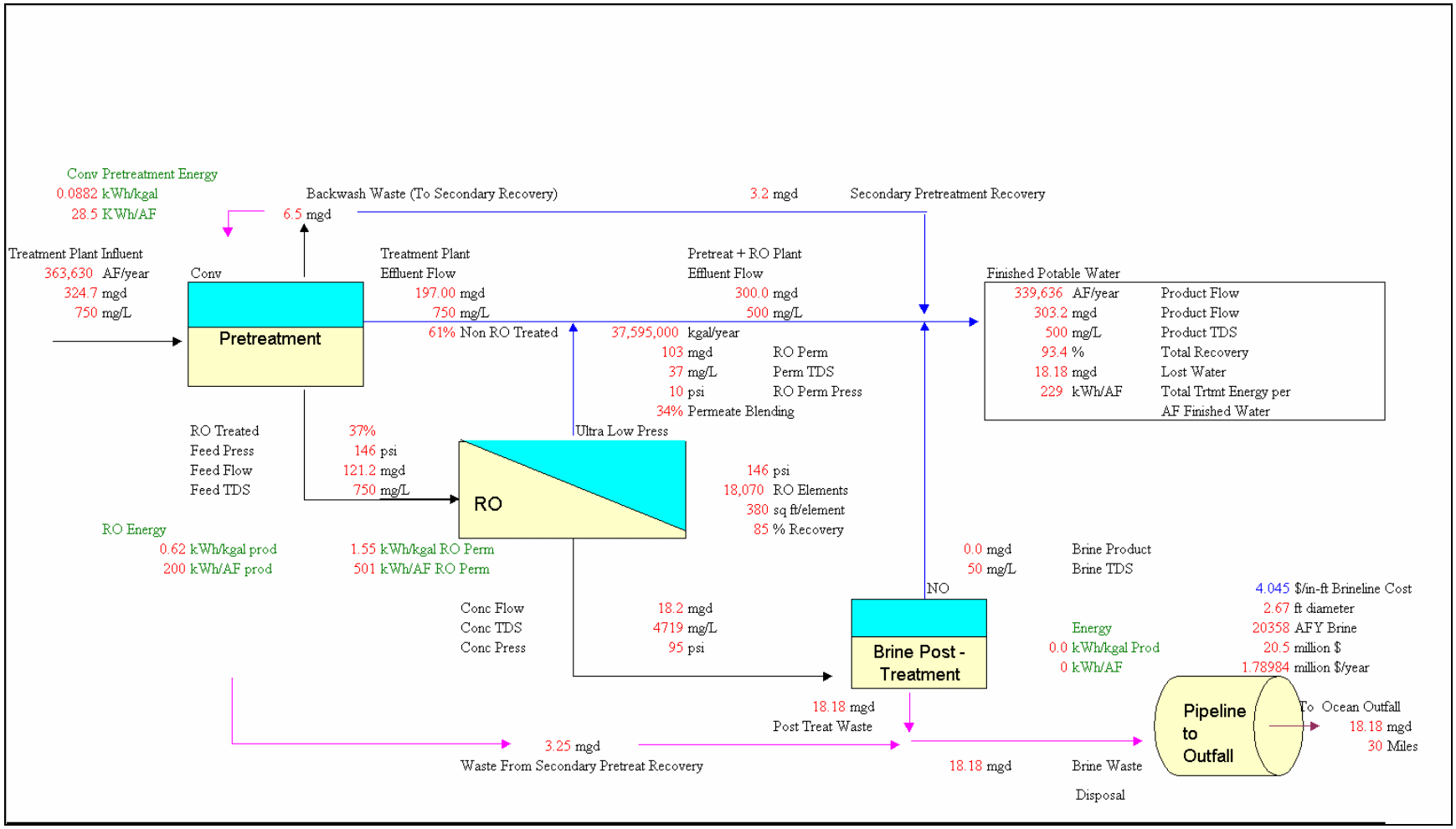

Figure 4. Large-scale, split-flow desalination cost model

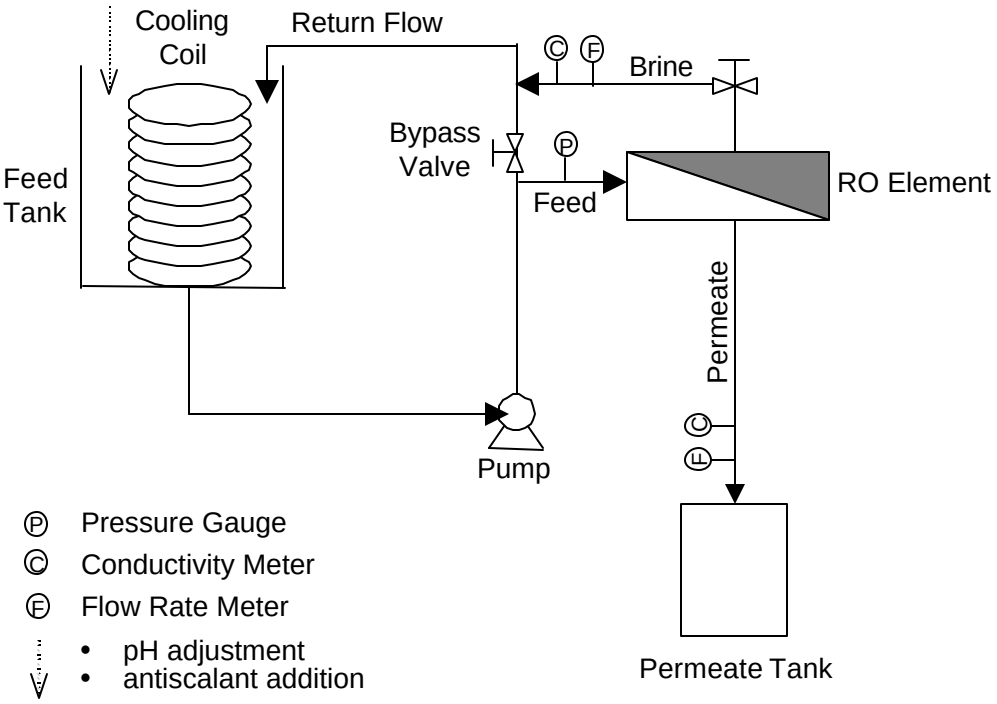

Figure 5. Schematic drawing of bench-scale membrane test unit

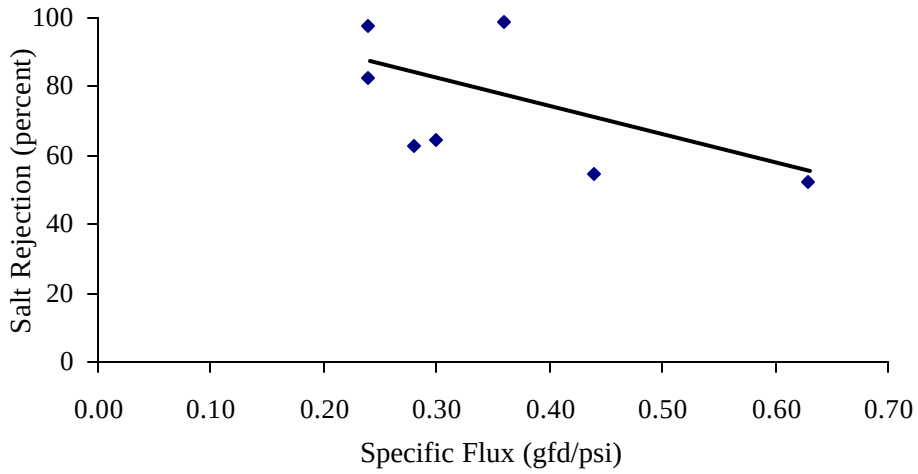

Figure 6. Relationship of specific flux and salt rejection for nanofiltration membranes

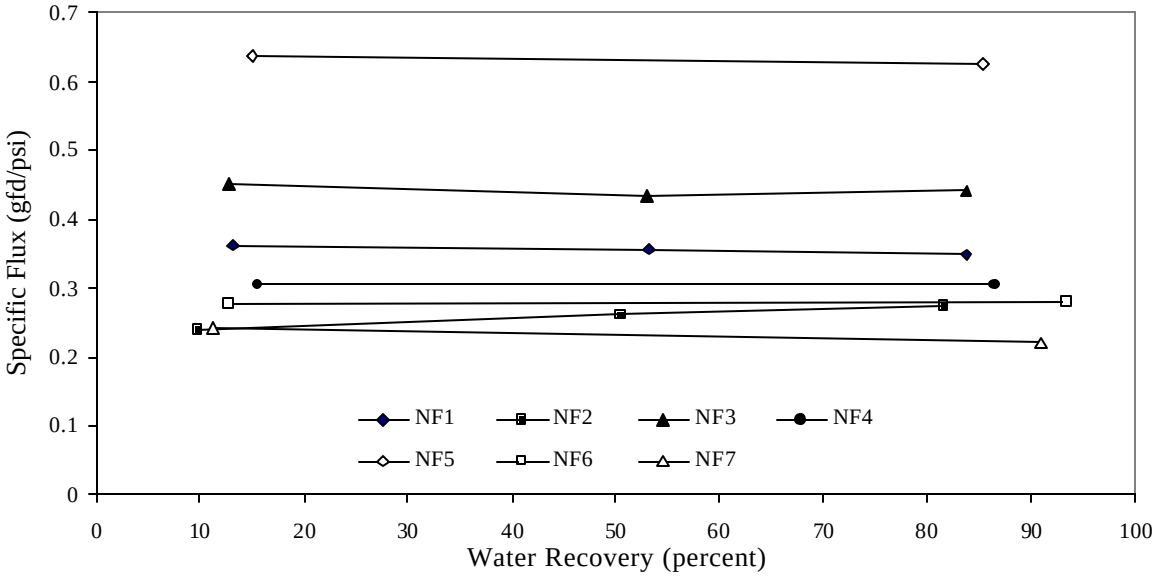

Figure 7. Effect of water recovery on nanofiltration membrane flux

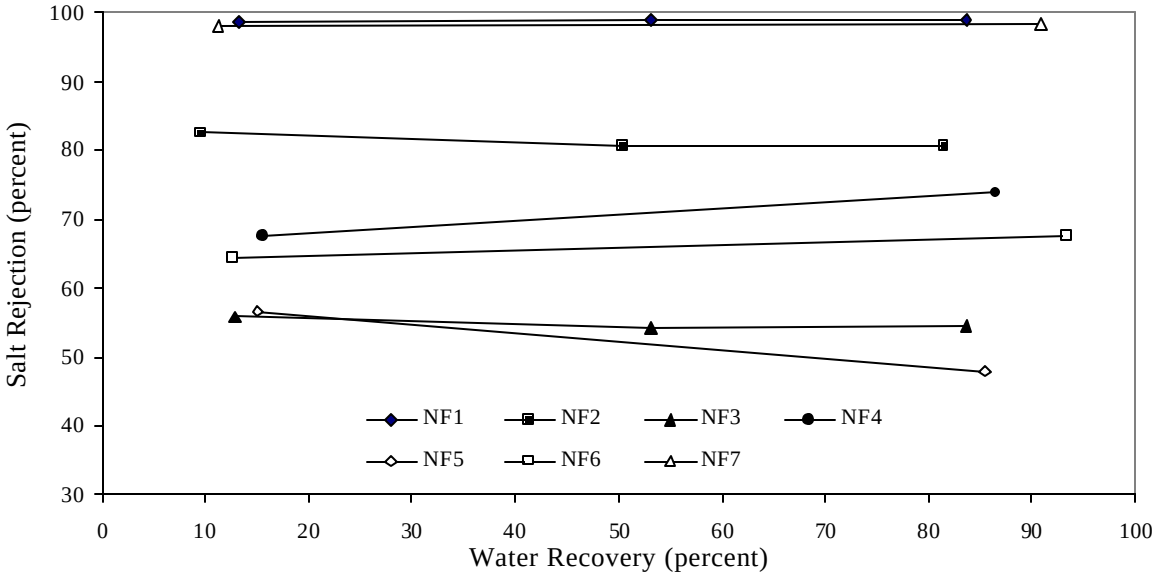

Figure 8. Effect of water recovery on nanofiltration membrane rejection

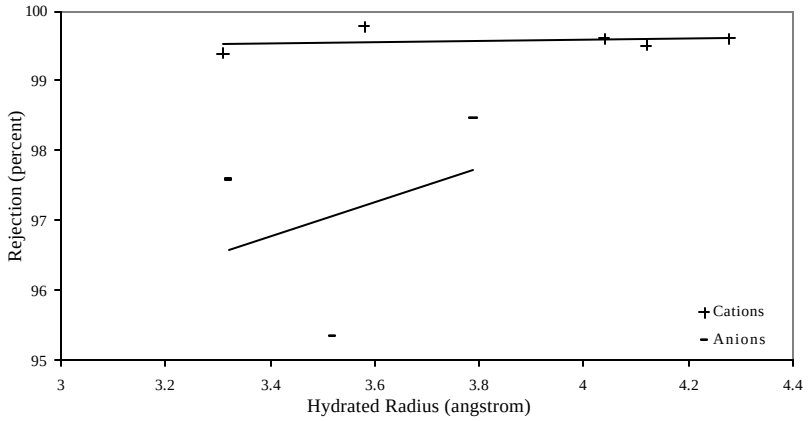

(a)

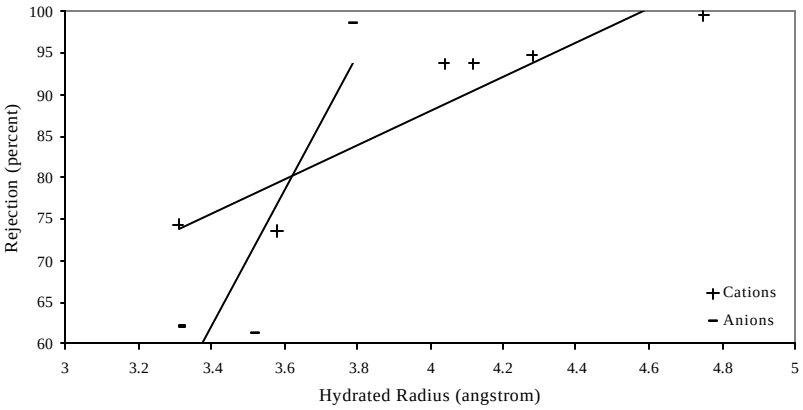

(b)

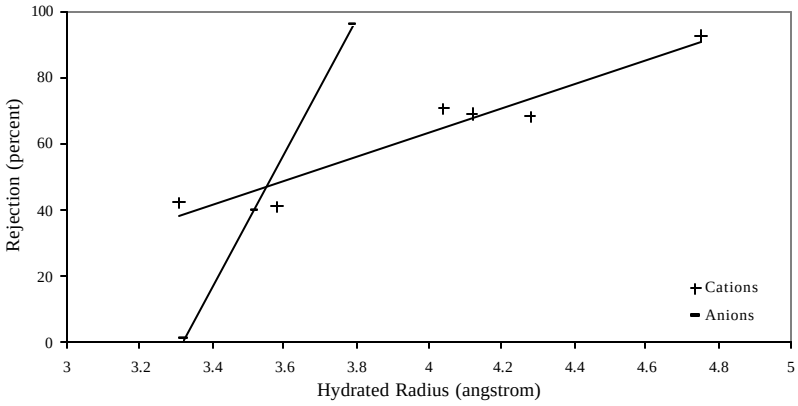

(c)

Figure 9. Effect of hydrated radius on nanofiltration membrane salt rejection: (a) NF1, (b) NF2, (c) NF3

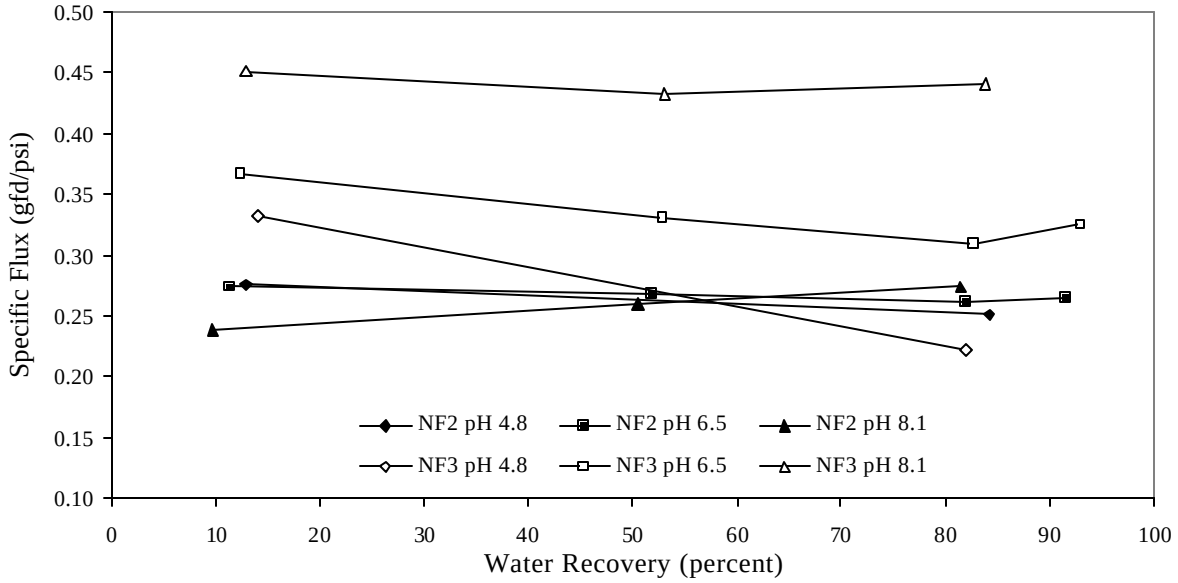

Figure 10. Effect of pH on membrane flux

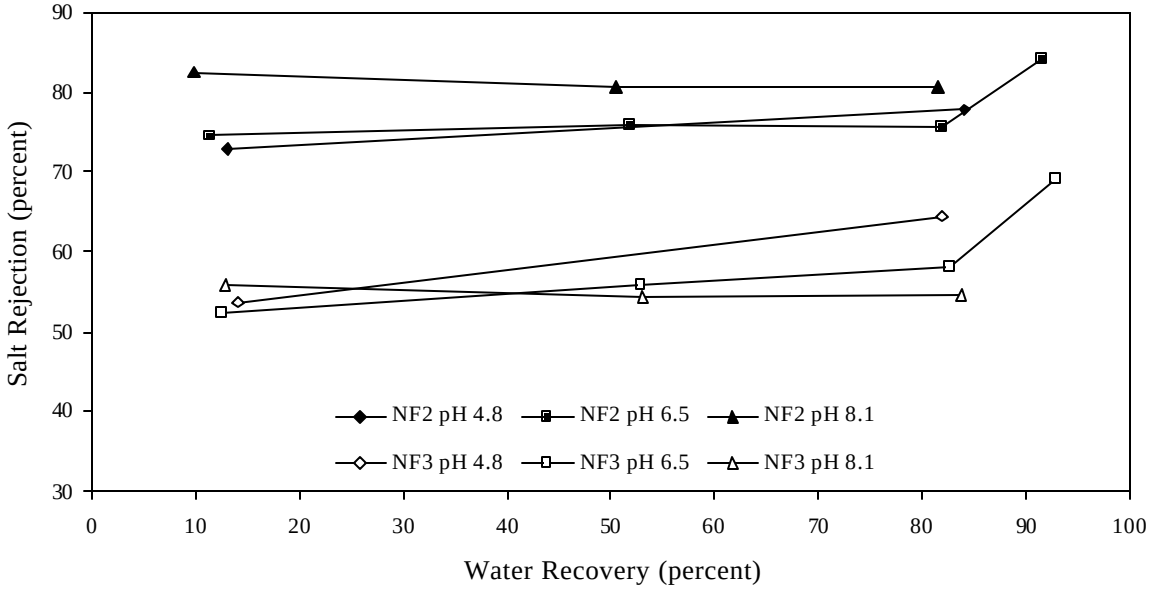

Figure 11. Effect of pH on salt rejection

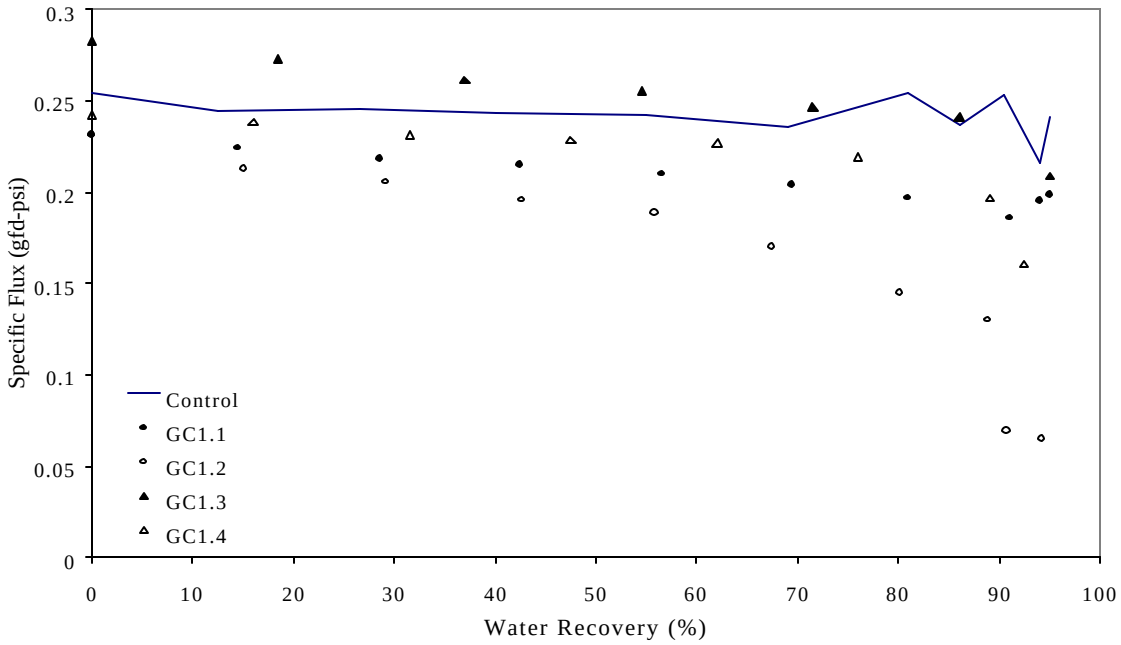

Data normalized to 25°C

Figure 12. Specific permeate flux for citric acid using CRW/SPW

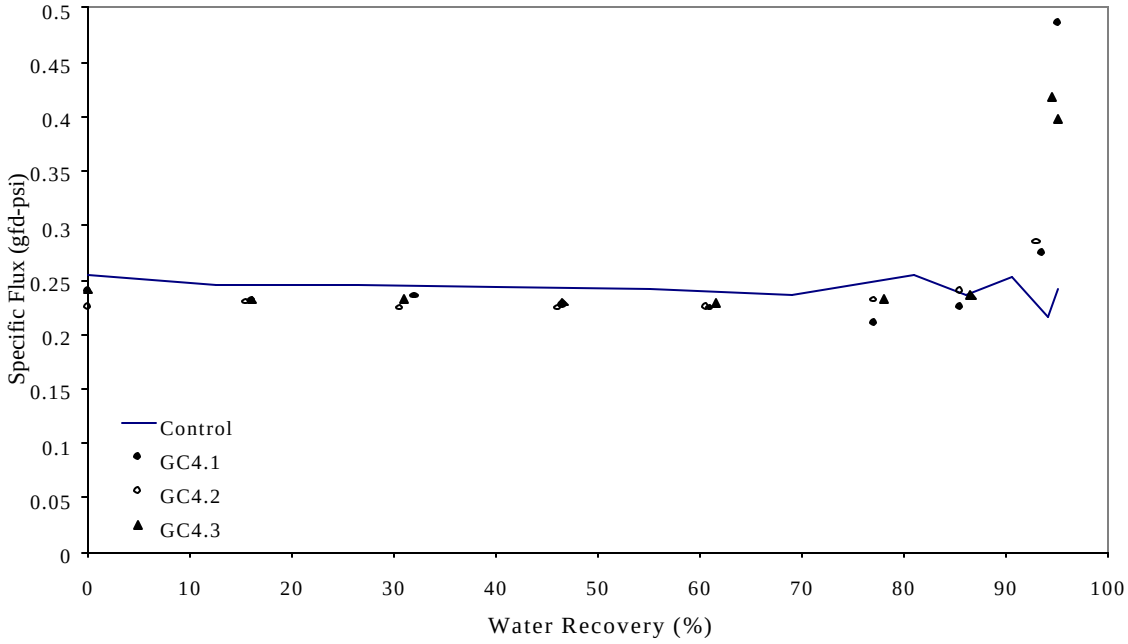

Data normalized to 25°C

Figure 13. Specific permeate flux for salicylic acid using CRW/SPW

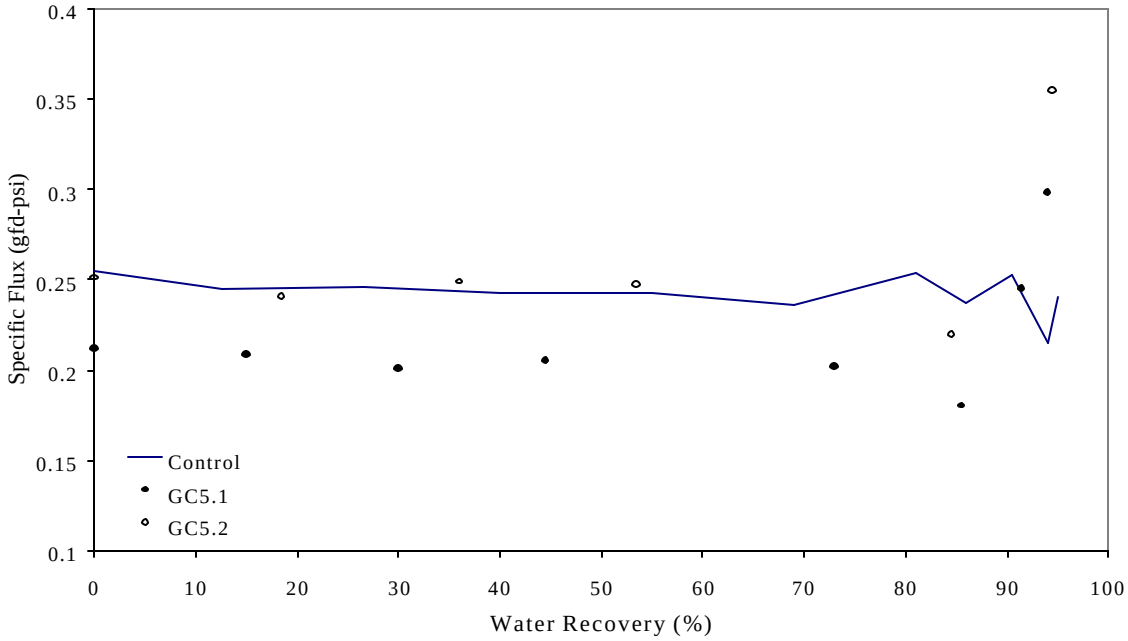

Data normalized to 25°C

Figure 14. Specific permeate flux for EDTA using CRW/SPW

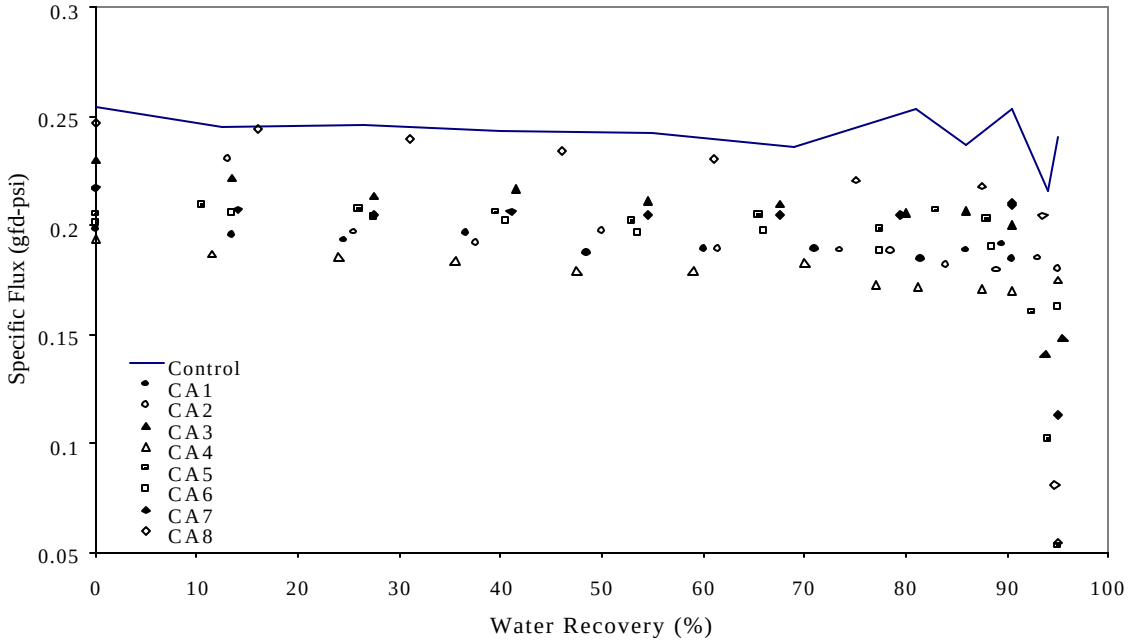

Data normalized to 25°C

Figure 15. Specific permeate flux for commercial antiscalants using CRW/SPW

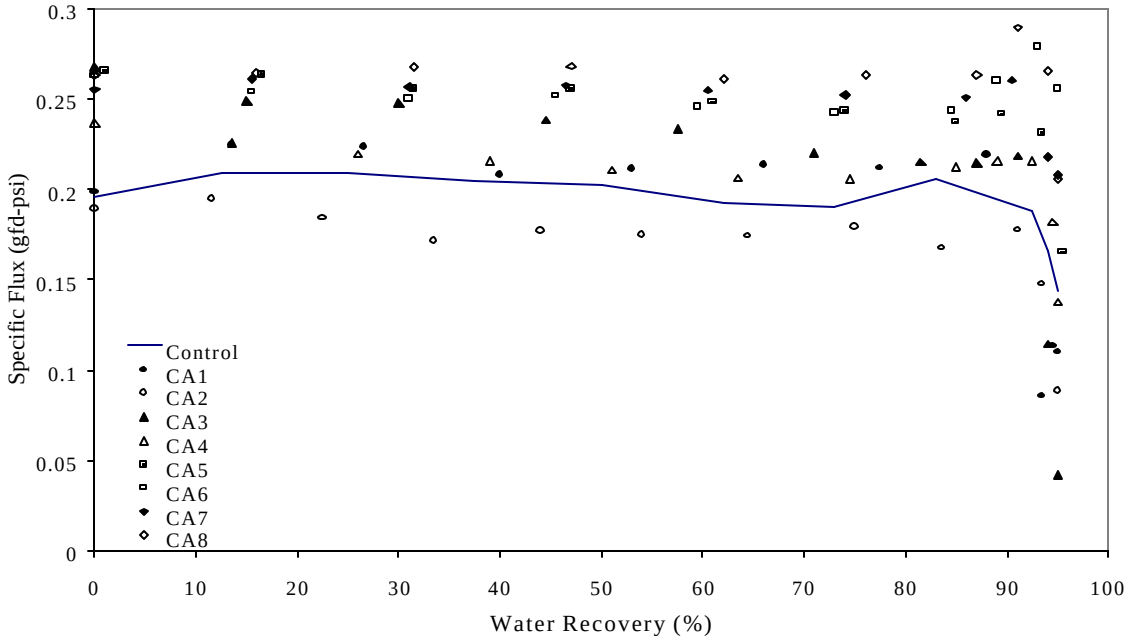

Data normalized to 25°C

Figure 16. Specific permeate flux for commercial antiscalants using CRW at pH 8.3

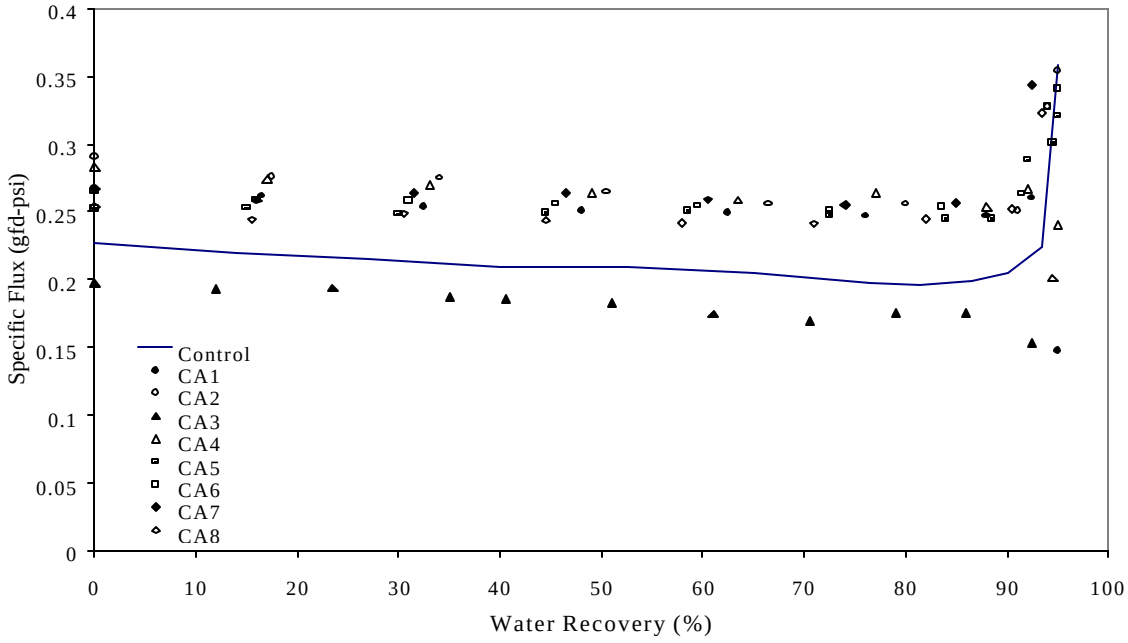

Data normalized to 25°C

Figure 17. Specific permeate flux for commercial antiscalants using CRW at pH 7.0

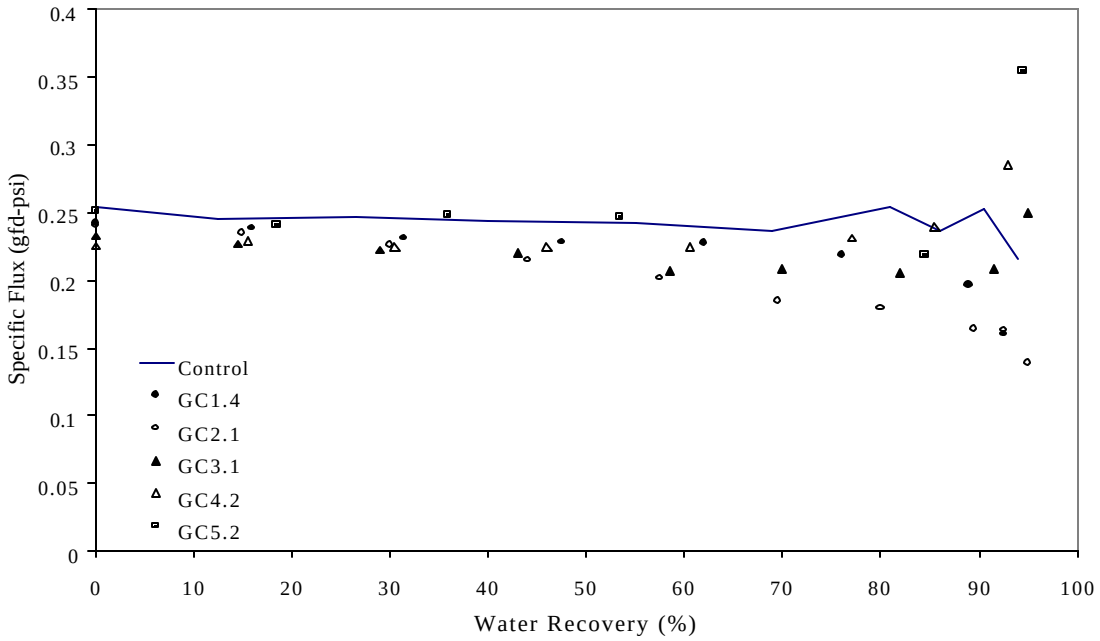

Data normalized to 25°C

Figure 18. Specific permeate flux for generic antiscalants using CRW/SPW

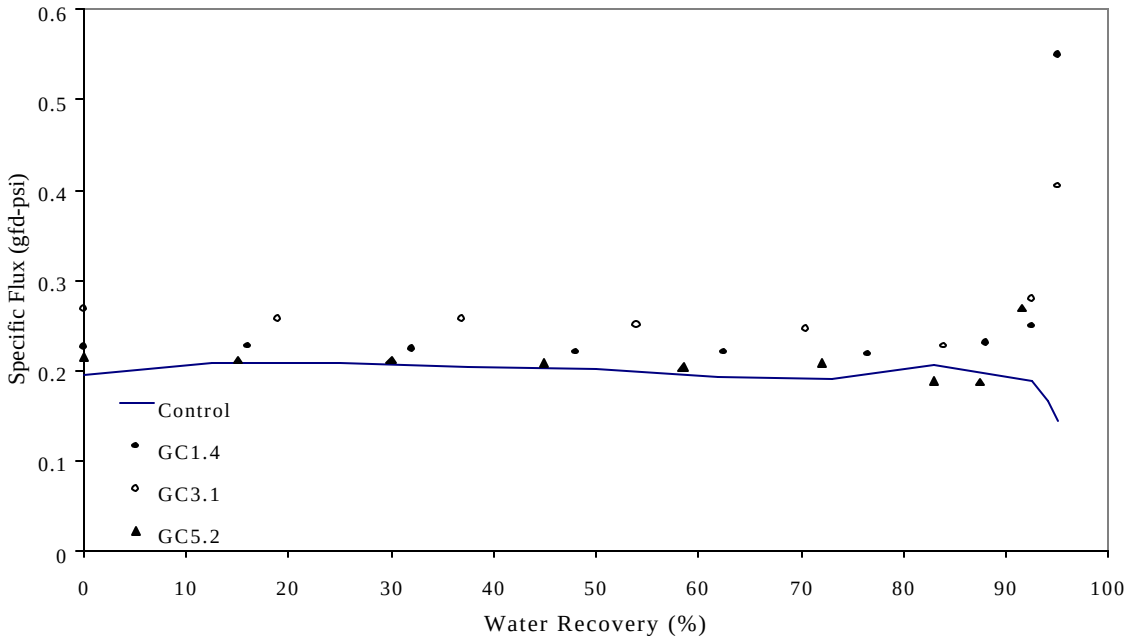

Data normalized to 25°C

Figure 19. Specific permeate flux for generic antiscalants using CRW at pH 8.3

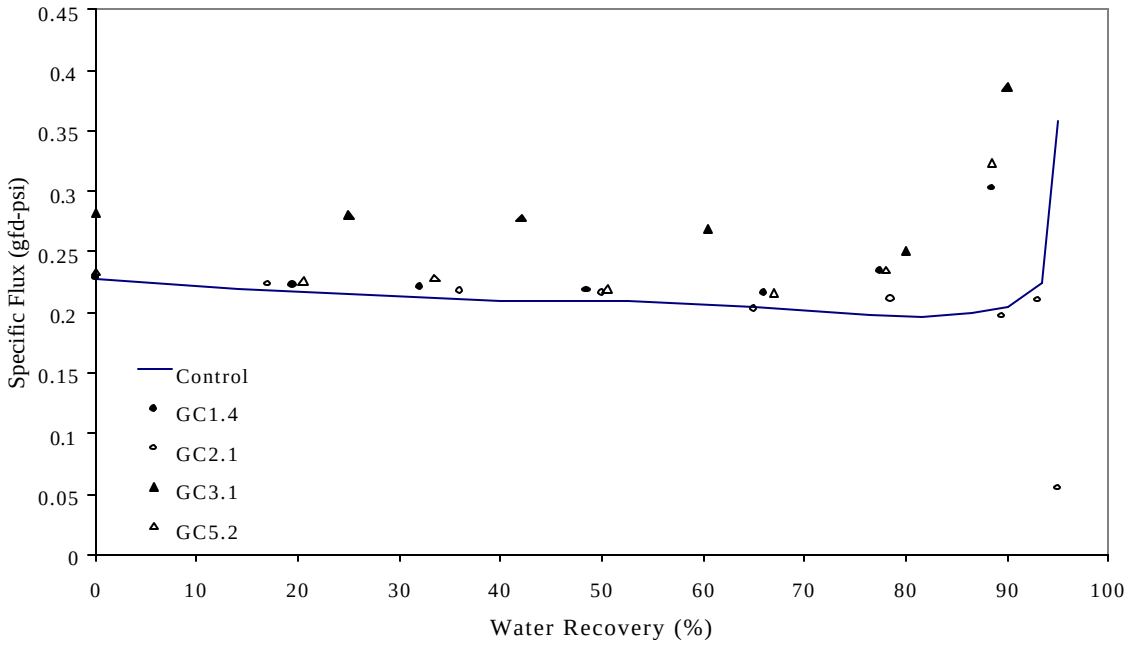

Data normalized to 25°C

Figure 20. Specific permeate flux for generic antiscalants using CRW at pH 7.0

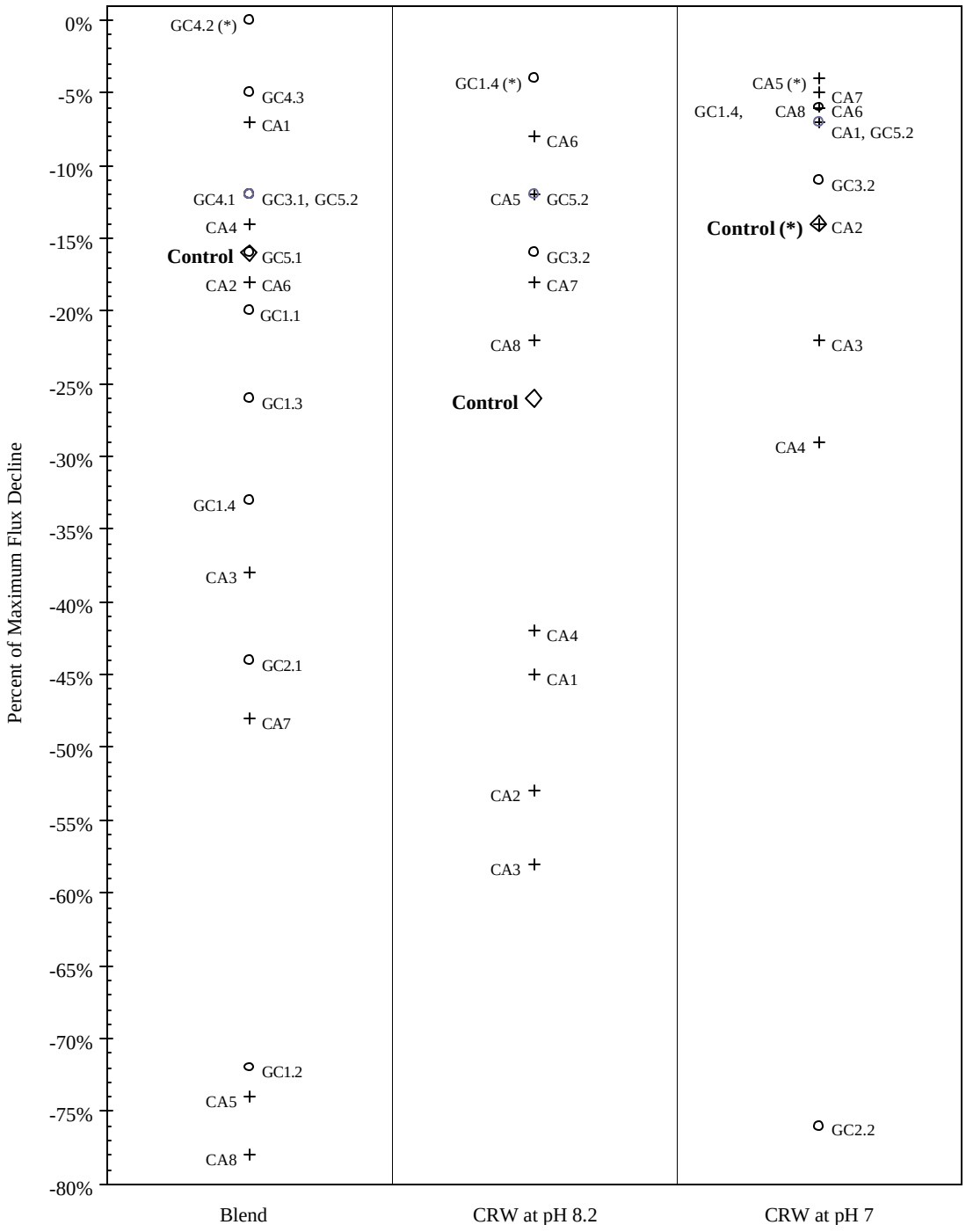

Figure 21. Maximum permeate flux decline of commercial and generic antiscalants in three types of waters in RO bench-scale testing. Data with (*) indicated that significant flux increase was observed at high water recovery.

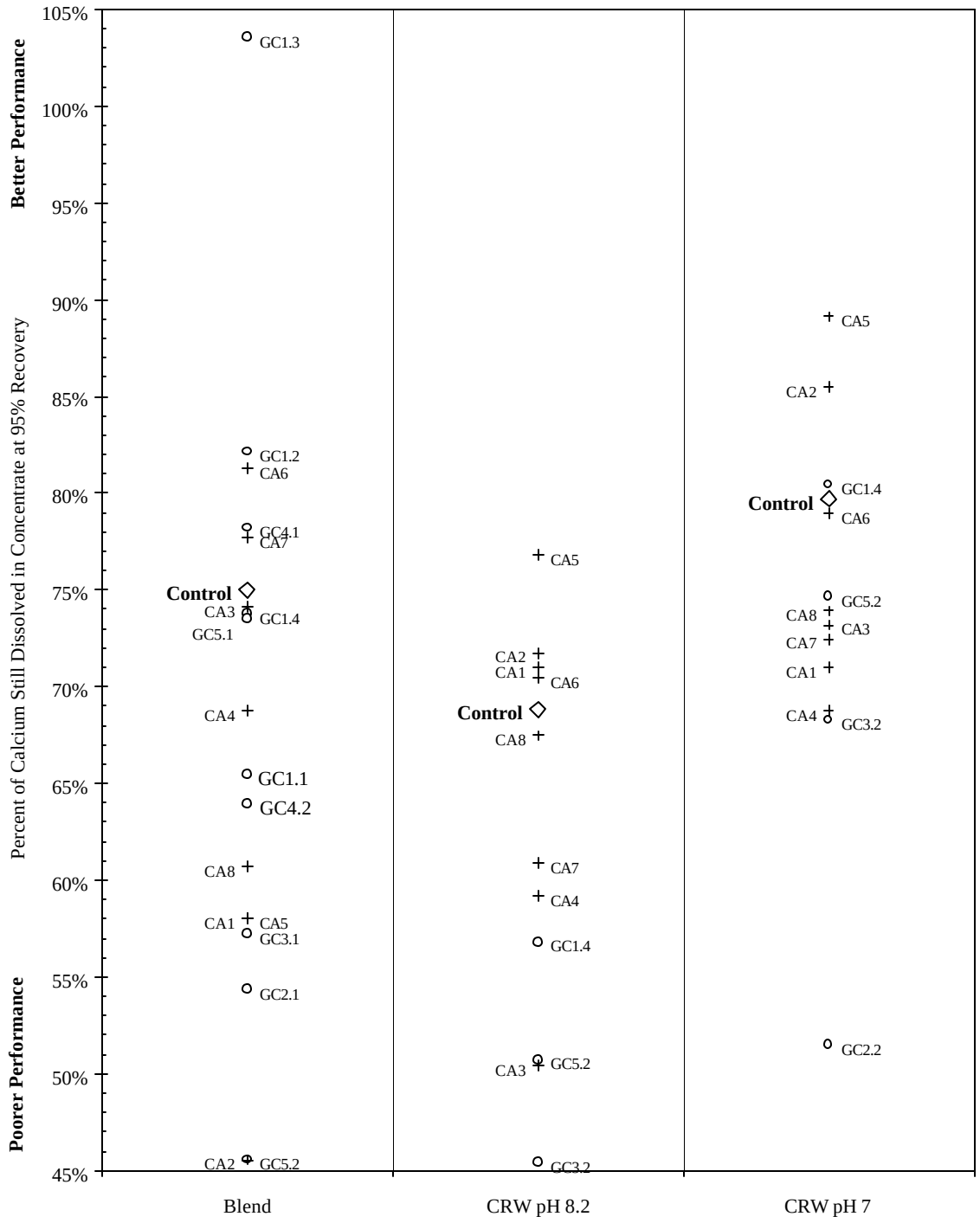

Figure 22. Dissolved calcium in RO concentrate for commercial and generic antiscalants in bench-scale testing.

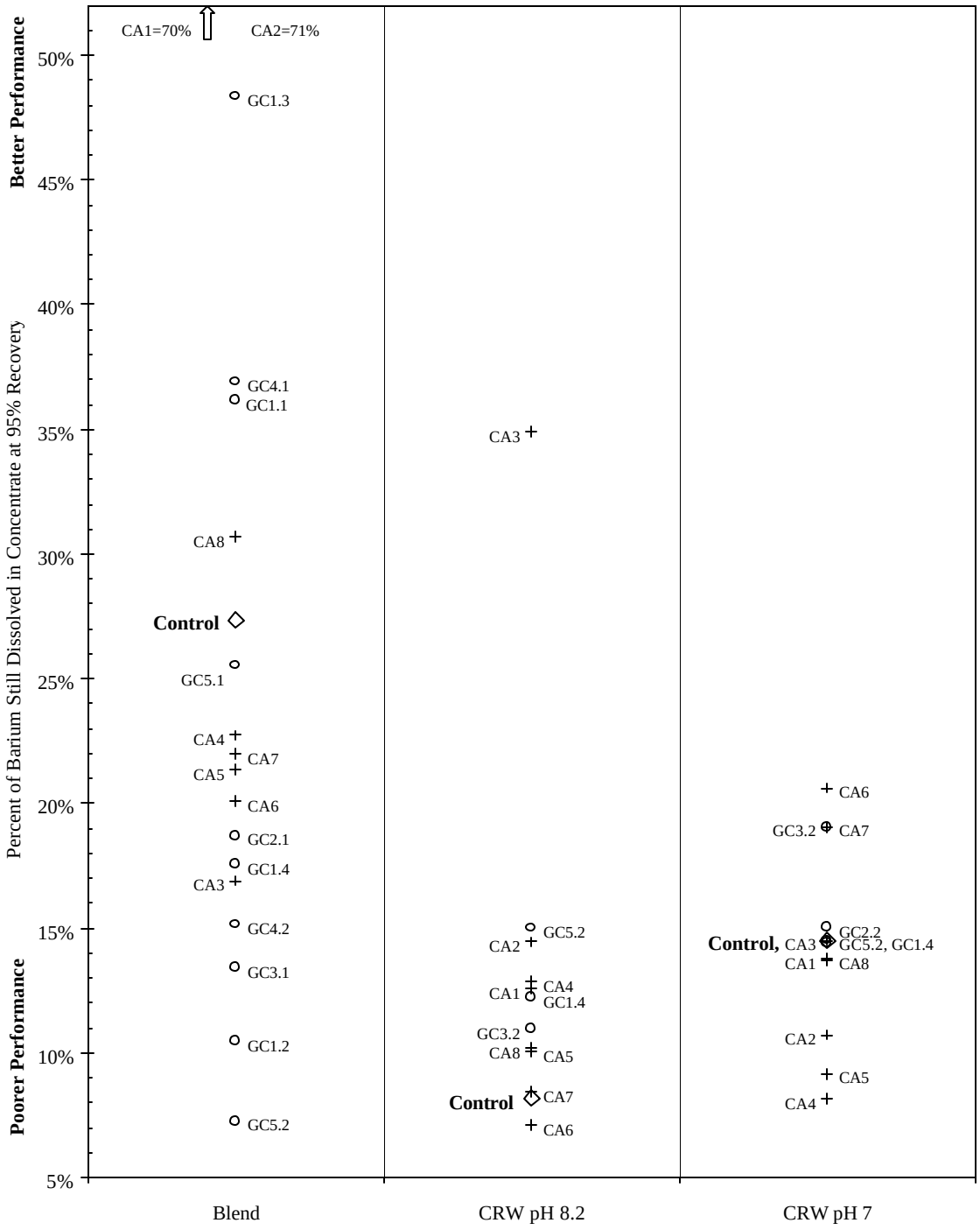

Figure 23. Dissolved barium in RO concentrate for commercial and generic antiscalants in bench-scale testing.

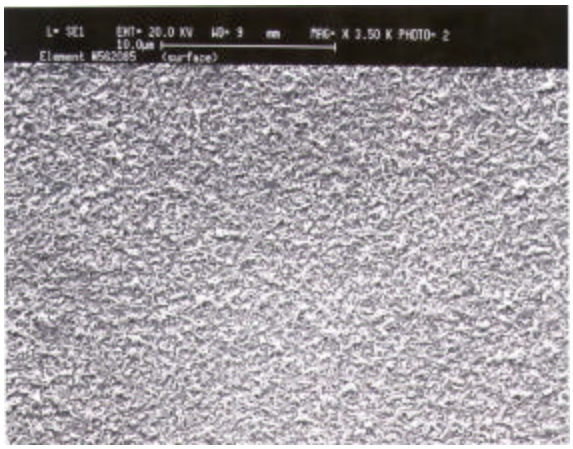

Figure 24. SEM micrograph of a cleaned reverse osmosis membrane

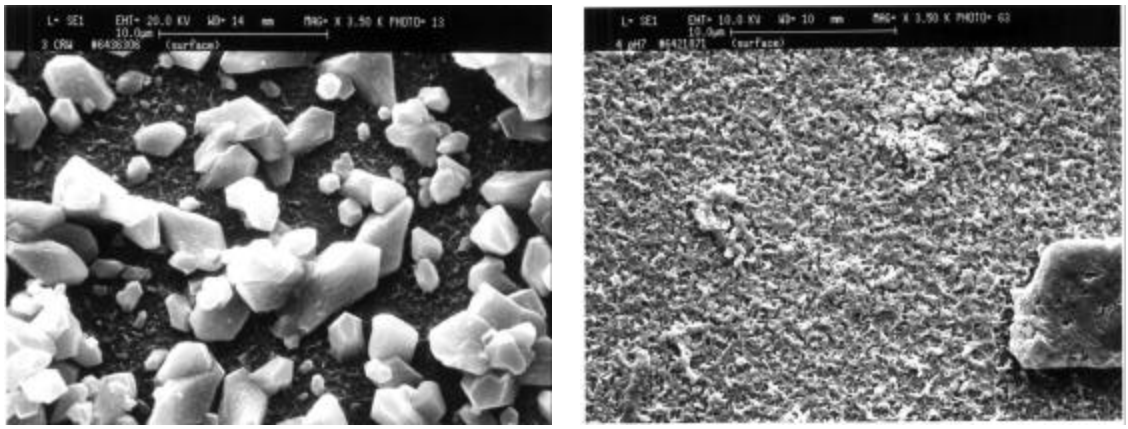

(a) (b)

Figure 25. Representative SEM micrographs of fouled reverse osmosis membranes from bench-scale testing: (a) inorganic scales, (b) organic fouling

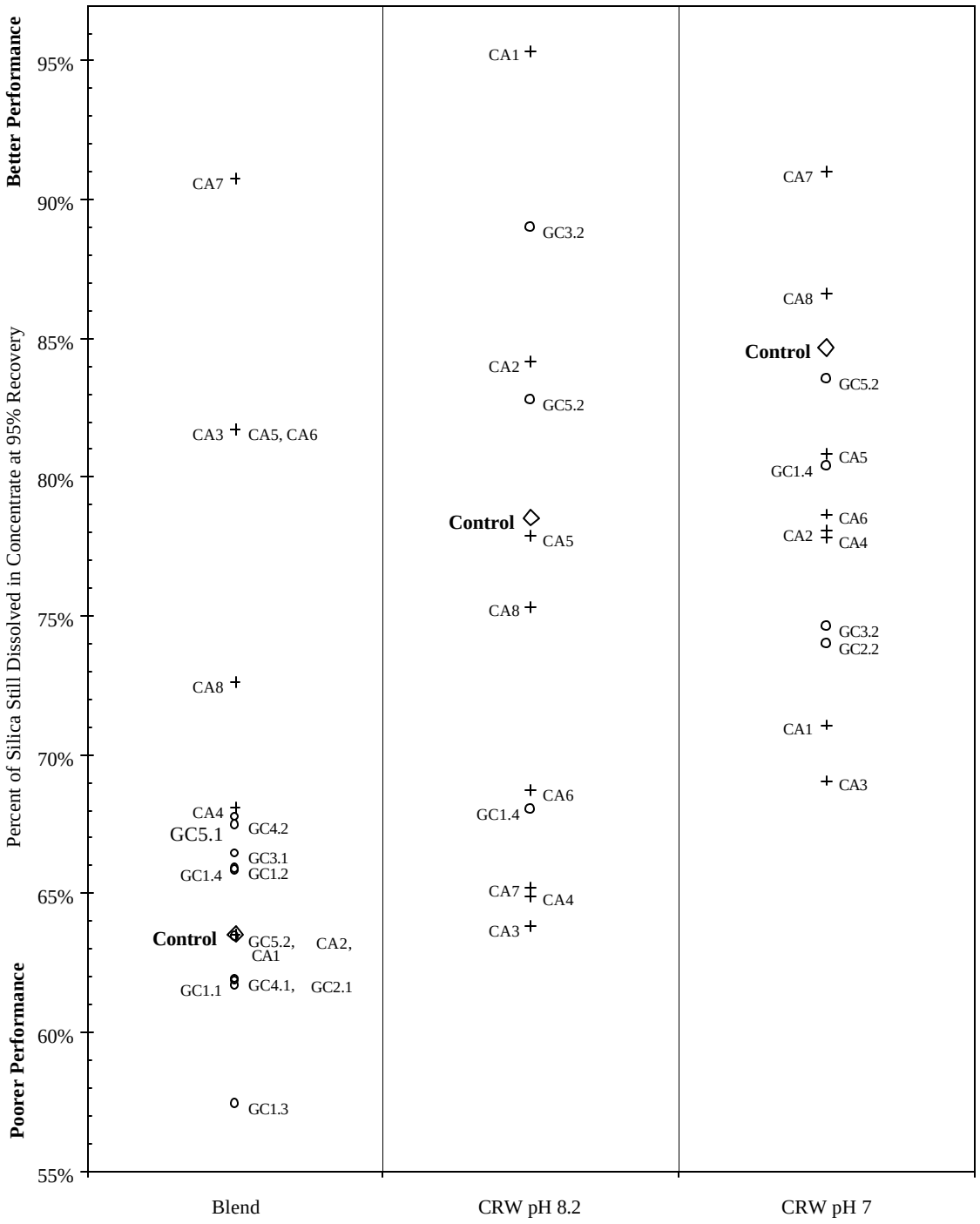

Figure 26. Dissolved silica in RO concentrate for commercial and generic antiscalants in bench-scale testing.

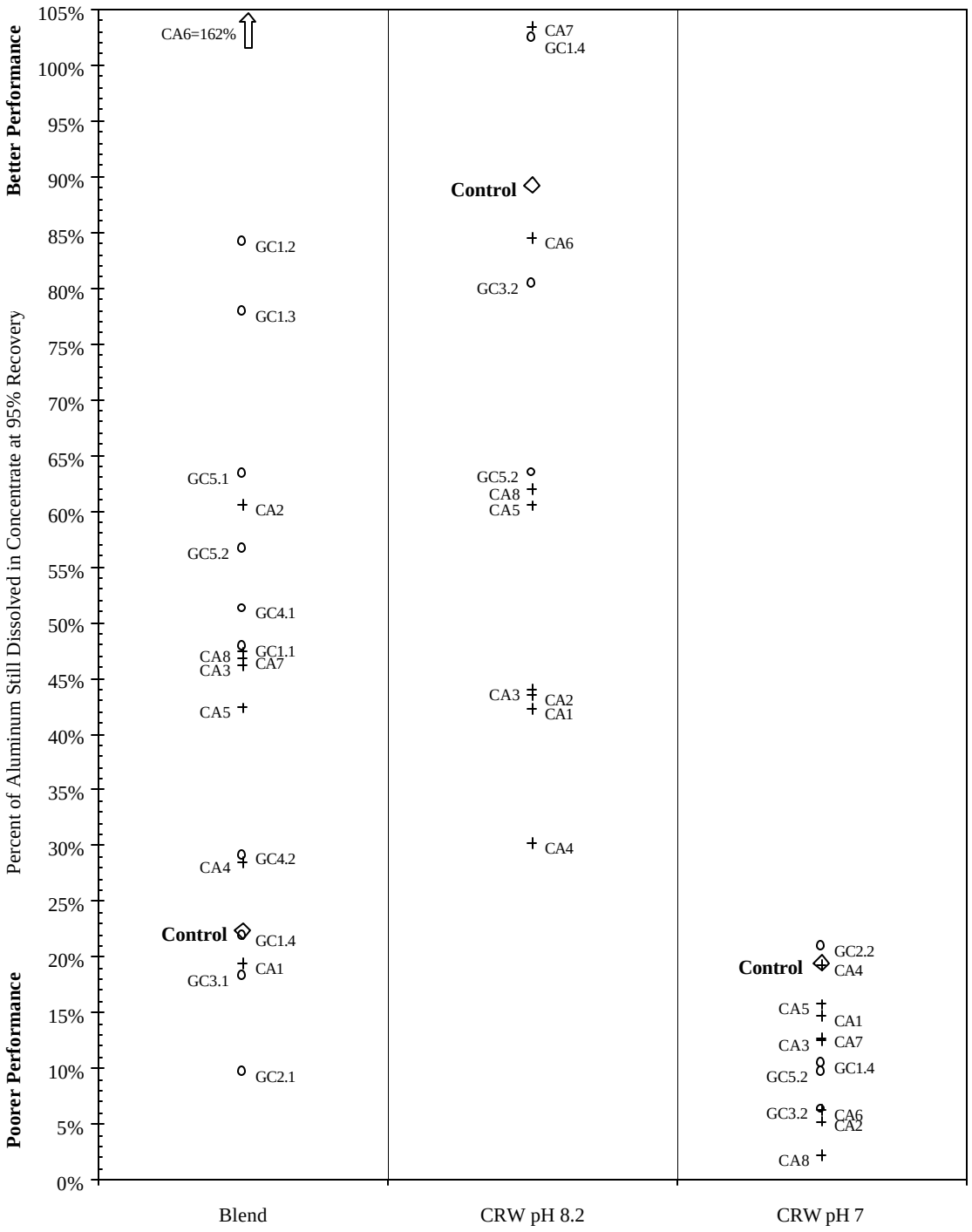

Figure 27. Dissolved aluminum in RO concentrate for commercial and generic antiscalants in bench-scale testing.

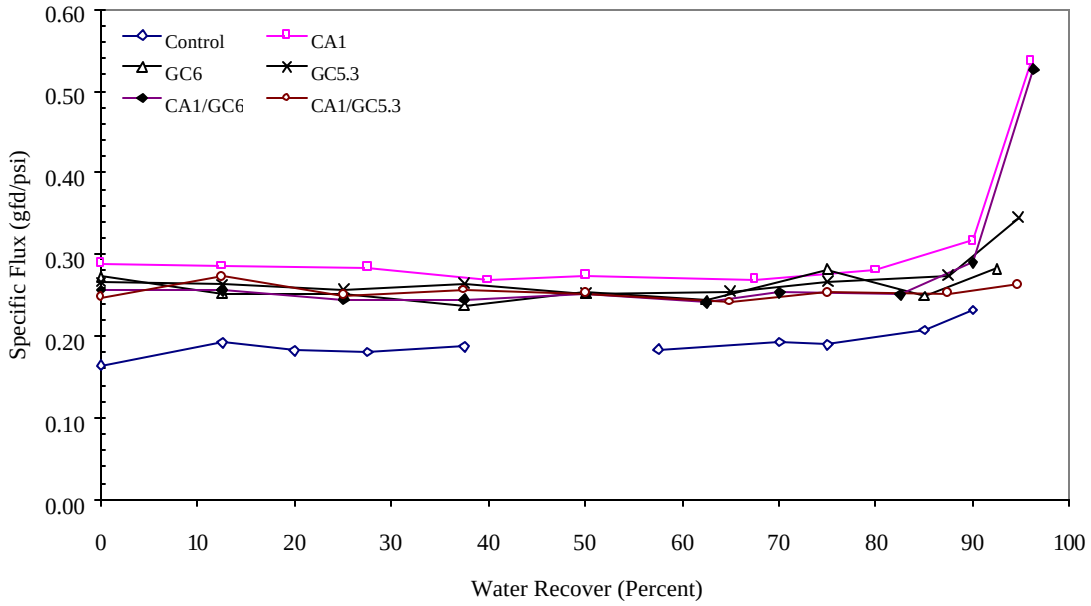

Figure 28. Specific permeate flux for commercial and generic antiscalants using CRW at pH 6.7 with 170 µg/L added aluminum

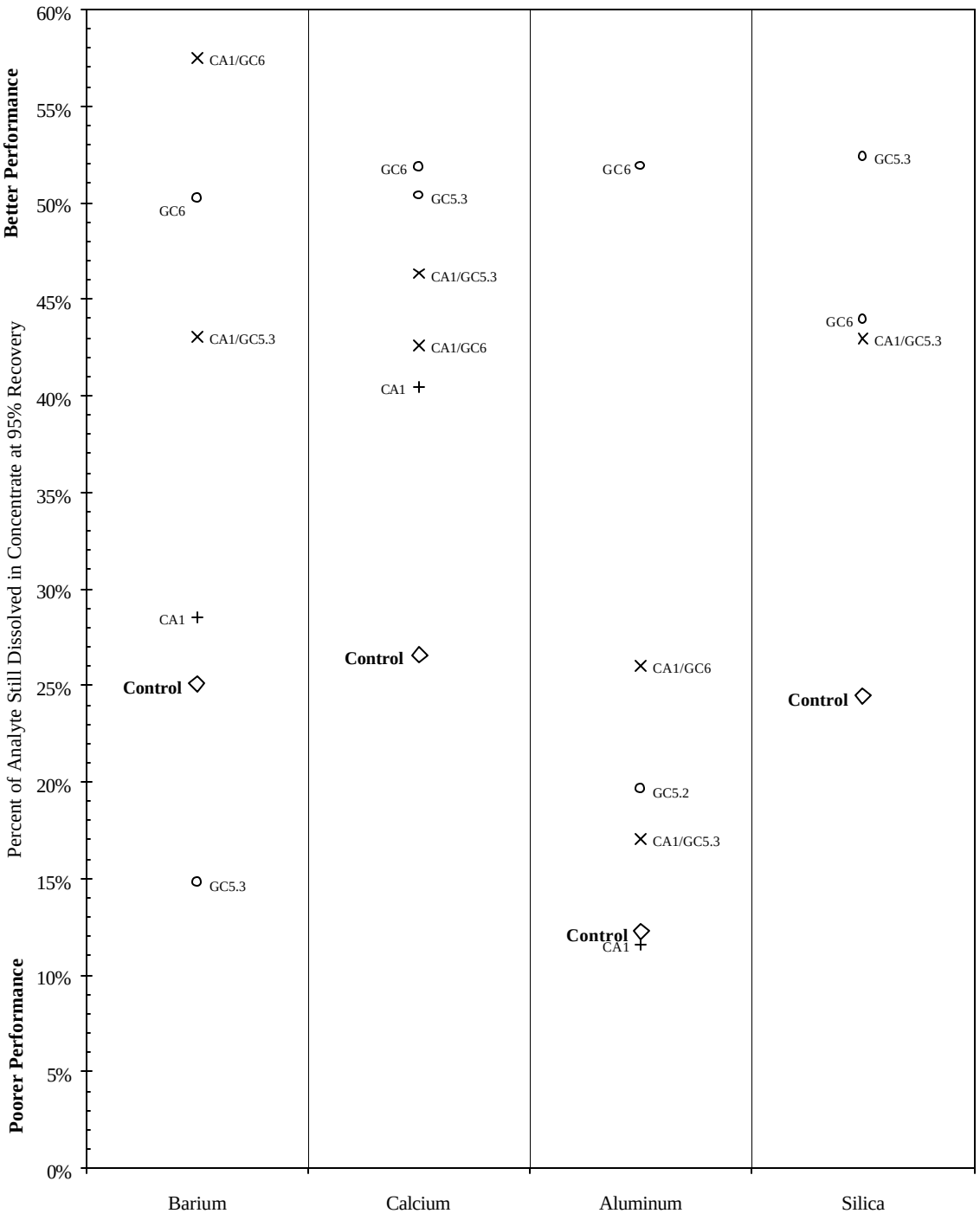

Figure 29. Dissolved analytes in RO concentrate for commercial, generic and blends of commercial and generic antiscalants in bench-scale testing with 170 µg/L added aluminum.

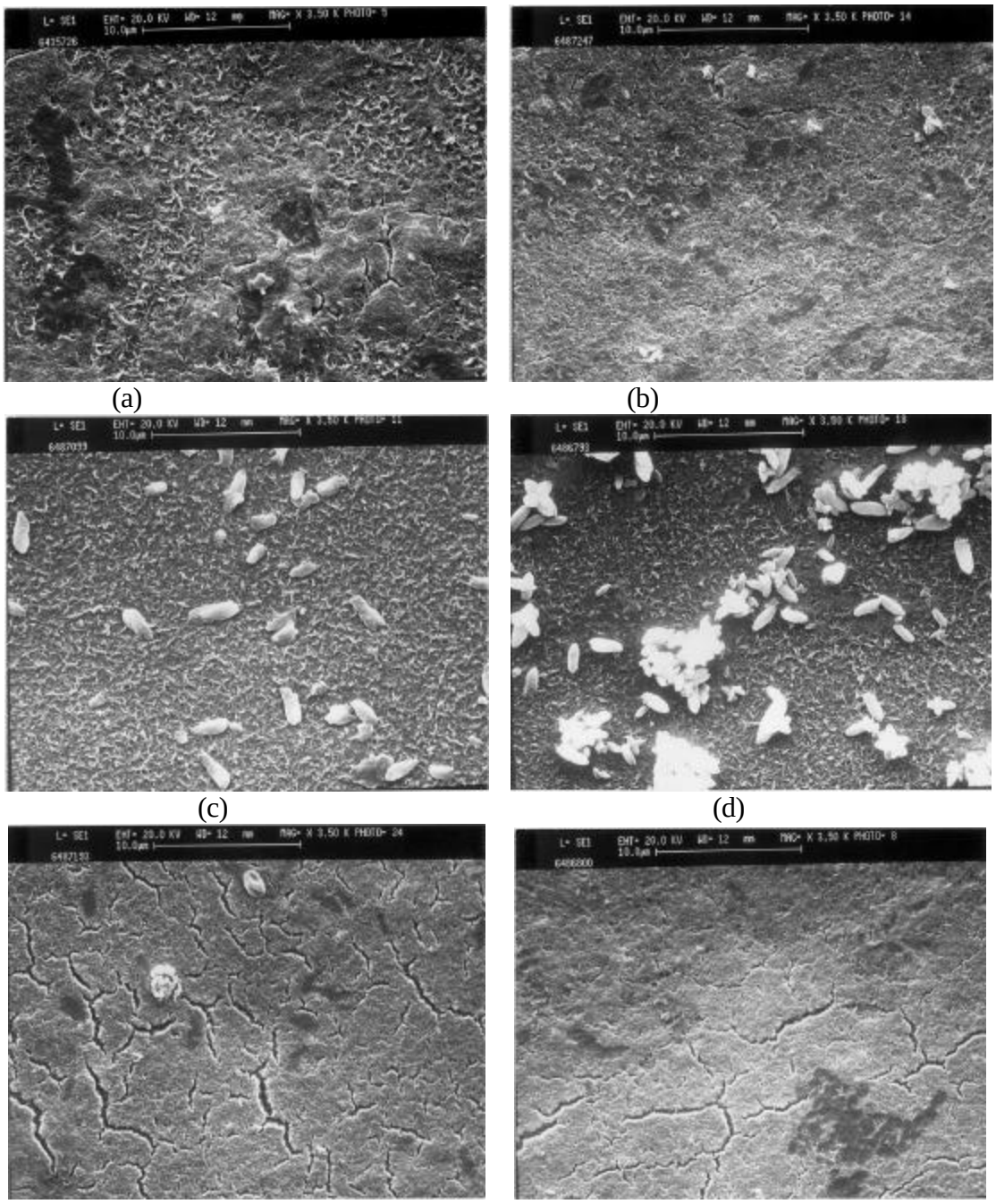

(a) (b)

(c) (d)

(e) (f)

Figure 30. SEM micrographs of fouled reverse osmosis membranes from the aluminum addition study: (a) Control, (b) CA1, (c) GC6, (d) GC5.3, (e) CA1/GC6, (f) CA1/GC5.3

APPENDIX A

All water quality sampling was conducted by Metropolitan's staff. Inorganic and microbial analyses were analyzed at Metropolitan's Water Quality Laboratory in La Verne, Calif. The water quality constituents were analyzed according to the methods described below. *Standard Methods for the Examination of Water and Wastewater* (APHA, AWWA, and WEF 1998) was referenced for sample analysis wherever possible.

Inorganic Constituents

Alkalinity and Hardness were analyzed by titration according to Standard Methods 2320B and 2340C (APHA, AWWA, and WEF 1998).

Total Dissolved Solids (TDS) was measured using Standard Method 2540C (APHA, AWWA, and WEF 1998) or estimated from conductivity measurements.

Bromide, Chloride, Fluoride, Nitrate, and Sulfate were analyzed using a modified EPA Method 300.0 and a Dionex Model DX300 ion chromatograph. The minimum reporting levels (MRL) for each constituent (in mg/L) are: Br: 0.02, Cl: 2.0, F: 0.02, NO_3: 0.05, and SO_4: 4.0.

Silica levels were determined according to Standard Method 4500-Si D (APHA, AWWA, and WEF 1998) using a Shimadzu UV-2401PC ultraviolet/visible spectrophotometer.

Boron was measured using the Curcumin method as absorbance at 540 nm on a spectrophotometer against a standard curve using Standard Method 4500-B (APHA, AWWA, and WEF 1998).

Calcium, Magnesium, Potassium, Sodium were analyzed according to Standard Method 3111B (APHA, AWWA, and WEF 1998) using a Varian SpectrAA-300/400 atomic absorption spectrophotometer. The MRL for this method is 0.1 mg/L for each constituent.

Aluminum, Arsenic, Iron, Manganese, Barium and Strontium (trace metals) were analyzed according to EPA Method 200.8 using a Perkin Elmer Elan 6000 ICP-MS.

MRLs for this method are as follows: Al: 5 µg/L, As: 0.5 µg/L, Fe: 20 µg/L; Mn: 5 µg/L; Ba: 5 µg/L, and Sr: 20 µg/L.

Total Organic Carbon (TOC) samples were analyzed by the ultraviolet/persulfate oxidation method (Standard Method 5310C, APHA, AWWA, and WEF 1998) using a Sievers 800 organic carbon analyzer. The MRL for this method is 0.05 mg/L.

Dissolved Organic Carbon (DOC) was defined by a filtration step involving a pre-washed 0.45 micron nylon membrane filter. DOC samples are analyzed by the ultraviolet/persulfate oxidation method (Standard Method 5310C, APHA, AWWA, and WEF 1998) using a Sievers 800 organic carbon analyzer. The MRL for this method is 0.05 mg/L.

Ultraviolet Light (UV) samples were analyzed at 254 nm using a Shimadzu UV-2401PC ultra-violet/visible spectrophotometer according to Standard Method 5910 (APHA, AWWA, and WEF 1995). Samples were filtered through a prewashed 0.45-µm Teflon membrane to remove turbidity which can interfere with UV measurement.

Free and Total Chlorine was measured using Standard Method 4500-Cl G (APHA, AWWA, and WEF 1998). For all free chlorine samples, 200 µl of 0.03 *N* thioacetamide solution per 10 mL of sample was added to control for interference by monochloramine.

Microbacteriological Methods

Heterotrophic Plate Count (HPC) bacteria were identified and enumerated using the R2A membrane filtration technique (plating in triplicate). R2A plates are incubated at 28ºC for 7 days, according to *Standard Methods* (APHA, AWWA, and WEF 1998).

Total Coliforms and *E. Coli.* were identified and enumerated according to *Standard Methods* (APHA, AWWA, and WEF 1998). Pretreatment influent and RO concentrate samples were analyzed using multiple tube fermentation methods and pretreatment effluent and RO permeate streams were analyzed using the membrane filtration option per *Standard Methods*.

APPENDIX B

In order to assess the performance of the pretreatment and salinity reduction steps, several key values were calculated based on raw process data. These calculated values include silt density index (SDI) for the pretreatment step and specific normalized flux, salt passage, and energy consumption for the RO system. These values were calculated using the following methods:

Specific Ultra Violet Light Absorbance at 254 nm (SUVA) was calculated by dividing the measured UV light absorbance at 254 nm (m^{-1}) by the measured TOC (mg/L) and multiplying by 100.

Silt Density Index (SDI) was measured using the method described by the American Society for Testing and Materials (ASTM) method D4189-82. The initial time (t_o) and the time after 15 minutes of continuous flow (t_{15}) to collect 500 ml through a 0.45 μm Millipore filter (Type HA, Millipore Corp., Bedford, Mass.) at 30 psig were measured. SDI was calculated using Equation 2.1:

$$SDI = \left[\frac{1 - \frac{t_o}{t_{15}}}{15} \right] * 100$$

where t_o = initial time in seconds to collect 500 ml

t_{15} = time in seconds to collect 500 ml after 15 minutes

Specific flux was calculated by the following equations:

Specific Flux = $(T_{Corr} * Q_{Permeate})/(a * P_{net})$ [gal/ft^2/day/psi]

where: T_{Corr} = Feed Temperature correction factor

$$T_{Corr} = e^{(U^* ((1/T) - (1/298))}$$

where: U = 3100 for Koch Fluid Systems ULP-TFC membranes

T = Measured temperature [°C]

$Q_{Permeate}$ = Permeate flow [gal/day]

a = Membrane surface area [ft^2]

$$P_{Net} = P_{Feed} - \Delta\pi - \Delta P_{Hydraulic} - P_{Permeate} \quad [psi]$$

where: $\Delta\pi$ = Differential osmotic pressure [psi]

$$\Delta\pi = 0.01 * (\Omega_{Average} - \Omega_{Permeate}) * (K_{Feed} + K_{Brine})/2$$

where: K = Conversion factor from conductivity to TDS [(mg/L)/(µS/cm)]

Ω = Conductivity [µS/cm]

Salt rejection was calculated by the following equation:

Salt rejection = [1-(permeate TDS/feed TDS)] x 100